PHYSICAL REVIEW D **83,** 053003 (2011)

Proper eighth-order vacuum-polarization function and its contribution to the tenth-order lepton $g-2$

T. Aoyama,[1,2] M. Hayakawa,[2,3] T. Kinoshita,[2,4] and M. Nio[2]

[1]*Kobayashi-Maskawa Institute for the Origin of Particles and the Universe (KMI), Nagoya University, Nagoya, 464-8602, Japan*
[2]*Theoretical Physics Laboratory, Nishina Center, RIKEN, Wako, 351-0198, Japan*
[3]*Department of Physics, Nagoya University, Nagoya, 464-8602, Japan*
[4]*Laboratory for Elementary Particle Physics, Cornell University, Ithaca, New York, 14853, USA*

(Received 12 January 2011; published 7 March 2011)

This paper reports the Feynman-parametric representation of the vacuum-polarization function consisting of 105 Feynman diagrams of the eighth order, and its contribution to the gauge-invariant set called Set I(i) of the tenth-order lepton anomalous magnetic moment. Numerical evaluation of this set is carried out using FORTRAN codes generated by an automatic code generation system GENCODEVPN developed specifically for this purpose. The contribution of diagrams containing an electron loop to the electron $g-2$ is $0.017\,47\,(11)(\alpha/\pi)^5$. The contribution of diagrams containing a muon loop is $0.000\,001\,67\,(3)(\alpha/\pi)^5$. The contribution of a tau-lepton loop is negligible at present. The sum of all these terms is $0.017\,47\,(11)(\alpha/\pi)^5$. The contribution of diagrams containing an electron loop to the muon $g-2$ is $0.0871\,(59)(\alpha/\pi)^5$. This is to be compared with the unpublished asymptotic analytic result $(0.252\,37 + O(m_e/m_\mu))(\alpha/\pi)^5$. The contribution of a tau-lepton loop to a_μ is $0.000\,237\,(1)(\alpha/\pi)^5$. The total contribution to a_μ, the sum of these terms and the mass-independent term, is $0.1048\,(59)(\alpha/\pi)^5$.

DOI: 10.1103/PhysRevD.83.053003 PACS numbers: 13.40.Em, 06.20.Jr, 12.20.Ds, 14.60.Cd

I. INTRODUCTION

The anomalous magnetic moment $g-2$ of the electron has played the central role in testing the validity of quantum electrodynamics (QED) as well as the standard model. The latest measurement of $a_e \equiv (g-2)/2$ by the Harvard group has reached the precision of 0.24×10^{-9} [1,2]:

$$a_e(\mathrm{HV08}) = 1\,159\,652\,180.73\,(0.28) \times 10^{-12} \qquad [0.24\ \mathrm{ppb}]. \tag{1}$$

At present the best prediction of theory consists of QED corrections of up to the eighth order [3–5], and hadronic corrections [6–12] and electroweak corrections [13–15] scaled down from their contributions to the muon $g-2$. To compare the theoretical prediction with the experiment (1), we also need the value of the fine structure constant α determined by a method independent of $g-2$. The best value of such an α has been obtained recently from the measurement of h/m_{Rb}, the ratio of the Planck constant and the mass of the Rb atom, combined with the very precisely known Rydberg constant and m_{Rb}/m_e [16]:

$$\alpha^{-1}(\mathrm{Rb10}) = 137.035\,999\,037\,(91) \qquad [0.66\ \mathrm{ppb}]. \tag{2}$$

With this α the theoretical prediction of a_e becomes

$$a_e(\mathrm{theory}) = 1\,159\,652\,181.13\,(0.11)(0.37)(0.77) \times 10^{-12}, \tag{3}$$

where the first, second, and third uncertainties come from the calculated eighth-order QED term, the tenth-order estimate, and the fine structure constant (2), respectively. The theory (3) is thus in good agreement with the experiment (1),

$$a_e(\mathrm{HV08}) - a_e(\mathrm{theory}) = -0.40\,(0.88) \times 10^{-12}, \tag{4}$$

proving that QED (standard model) is in good shape even at this very high precision.

An alternative test of QED is to compare the α of (2) with the value of α determined from the experiment and theory of $g-2$:

$$\alpha^{-1}(a_e08) = 137.035\,999\,085\,(12)(37)(33) \qquad [0.37\ \mathrm{ppb}], \tag{5}$$

where the first, second, and third uncertainties come from the eighth-order QED term, the tenth-order estimate, and the measurement of $a_e(\mathrm{HV08})$, respectively. Although the uncertainty of $\alpha^{-1}(a_e08)$ in (5) is a factor 2 smaller than $\alpha^{-1}(\mathrm{Rb10})$, it is not a firm factor since it depends on the estimate of the tenth-order term, which is only a crude guess [17]. For a more stringent test of QED, it is obviously necessary to calculate the actual value of the tenth-order term. In anticipation of this challenge we launched a systematic program several years ago to evaluate the complete tenth-order term [18–20].

The tenth-order QED contribution to the anomalous magnetic moment of the electron can be written as

$$a_e^{(10)} = \left(\frac{\alpha}{\pi}\right)^5 [A_1^{(10)} + A_2^{(10)}(m_e/m_\mu) + A_2^{(10)}(m_e/m_\tau) + A_3^{(10)}(m_e/m_\mu, m_e/m_\tau)], \tag{6}$$

where the electron-muon mass ratio $m_e/m_\mu = 4.836\,331\,71\,(12) \times 10^{-3}$ and the electron-tau mass ratio

 © 2011 American Physical Society

$m_e/m_\tau = 2.875\,64(47) \times 10^{-4}$ [17]. The contribution to the mass-independent term $A_1^{(10)}$ may be classified into six gauge-invariant sets, further divided into 32 gauge-invariant subsets depending on the nature of the closed lepton loop subdiagrams. Thus far, 24 gauge-invariant subsets which consist of 2785 vertex diagrams, have been evaluated and published [18,21–24]. Throughout the paper the overall factor $(\alpha/\pi)^5$ is omitted for simplicity.

In this paper we report the value of $A_1^{(10)}$ contributed by a subset, called Set I(i), which consists of 105 Feynman diagrams obtained by insertion of proper eighth-order vacuum-polarization diagrams in the second-order anomalous magnetic moment M_2. These diagrams can be represented by 39 independent integrals taking account of various symmetry properties. The evaluation of these integrals would be straightforward if the spectral function of the eighth-order vacuum polarization were known. Unfortunately, it is not available at present. Thus we follow an alternative approach of expressing the eighth-order vacuum-polarization function $\Pi^{(8)}(q^2)$ as a set of Feynman-parametric integrals and inserting them in the virtual photon line of the second-order anomalous magnetic moment M_2 [25].

Construction of the Feynman-parametric integral of the vacuum-polarization function and removal of subdiagram ultraviolet (UV) divergences by the K operation [25] are described in Sec. II. This scheme is implemented by an automated code generation system GENCODEVPN developed specifically for this purpose. Incorporation of $\Pi^{(8)}$ in M_2 is carried out in Sec. III. Since the K operation subtracts only the UV-divergent part of the renormalization constant, additional removal of UV-finite parts of renormalization constants must be carried out to obtain the standard on-the-mass-shell renormalization. This is shown explicitly in Sec. IV. Numerical evaluation of $M_{2,P_8}^{(ee)}$ is described in Sec. V, where the first e in the superscript (ee) refers to the open electron line and the second e refers to the closed electron loop. The contributions of the muon loop and tau-lepton loop to the electron $g-2$, namely, $M_{2,P_8}^{(em)}$ and $M_{2,P_8}^{(et)}$, are described in Sec. VI. The contribution of the Set I(i) diagrams to the muon $g-2$ is described in Sec. VII. Section VIII is devoted to the summary and discussion of this work. Especially, our result of the electron-loop contribution to the muon $g-2$ is compared to the prediction based on the renormalization group [26] and to the result obtained by the analytic-asymptotic expansion [27,28].

Appendix A describes the construction of Feynman-parametric integrals for M_{2,P_4^*}. Appendix B describes the on-shell renormalization scheme for the vacuum-polarization function. Appendix C gives intermediate renormalization of individual diagrams by the K operation. Appendix D gives the divergence structure of quantities of sixth or lower orders.

II. PARAMETRIC INTEGRAL OF VACUUM-POLARIZATION FUNCTION

Diagrams that contribute to the eighth-order vacuum-polarization can be classified into five types according to their structures (See Fig. 1). Contributions from the diagrams of Types f, g and h, and j to the tenth-order lepton $g-2$ have been evaluated previously in Refs. [3,21,22]. In this paper we focus our attention on the remaining Type i, a set of 105 proper eighth-order vacuum-polarization diagrams, which is the most complicated one of the diagrams shown in Fig. 1, and evaluate its tenth-order contribution Set I(i) to $g-2$.

A. Diagram representation

In order to deal with diagrams which contain closed lepton loops as well as open lepton paths, we have to

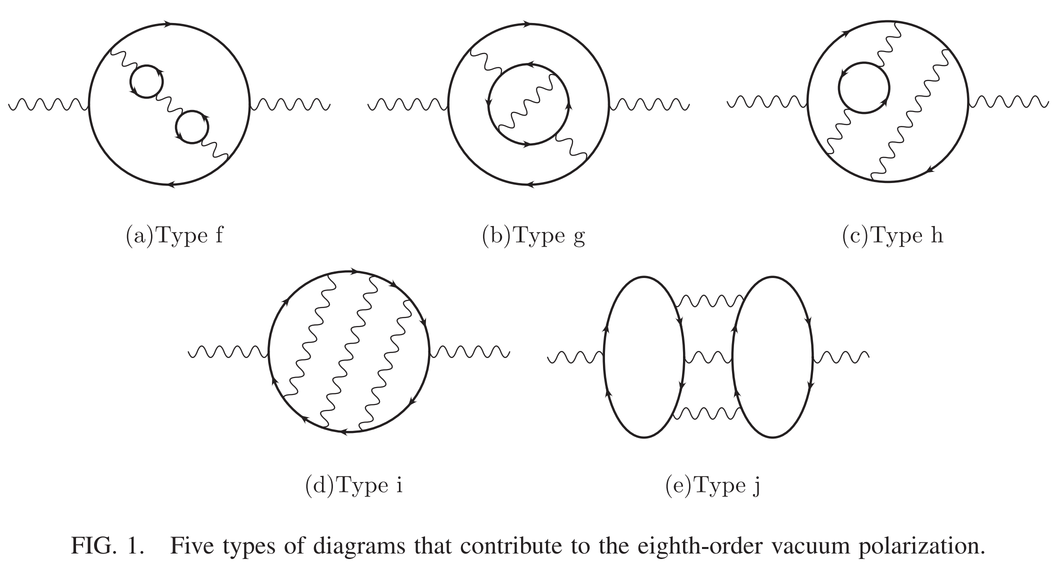

FIG. 1. Five types of diagrams that contribute to the eighth-order vacuum polarization.

generalize the rules for the diagrams without the closed lepton loop described in Ref. [19].

We begin by representing a diagram in terms of a sequence of symbols that characterize the photon lines by the following rules:

(1) Assign indices to photon lines, e.g., by lowercase alphabetical letters, "a," "b," ....
(2) Identify a vertex by the index of the photon line that is attached to the vertex.
(3) Read the indices of vertices along a lepton path (or loop) in a certain direction. (We adopt the reverse of the direction of the lepton propagator.)
(4) Enclose the sequences of indices of closed lepton loops by parentheses (but not indices of open lepton lines).

For example, the tenth-order diagram with two lepton loops shown in Fig. 2 [which belongs to Set I(g)] may be represented by a sequence, "ab(acbd)(cede)."

This representation is not unique because there are several possible choices of assignment of photon line indices, cyclic permutations of vertices along lepton loops, and permutations of lepton loops and paths. To reduce the ambiguity we adopt the convention that the sequence for the open lepton path comes first, followed by the lexicographical sequences of closed lepton loops. The sequence within a loop is chosen also lexicographically, e.g., the sequence (dacb) is rotated into (acbd). The photon line indices are taken from "a" in order of appearance in the sequence.[1]

For diagrams describing a vacuum-polarization loop, which is our main concern, we adopt an additional rule that the two photon lines external to the vacuum-polarization loop are labeled by "s" and "t," whose Lorentz indices are μ and ν, respectively. We also assume that the external momentum q flows in from the photon line "t" (ν) and leaves from the photon line "s" (μ). The sequence of lepton lines in the loop is chosen to start from the index "s."

B. Algorithm to generate a proper lepton loop diagram

We now present an algorithm for generating proper lepton loops of $2n$th order. A diagram of this type has a single lepton loop that consists of $2n$ vertices, $2n$ lepton lines, two external photon lines, and $(n-1)$ internal photon lines attached to the lepton loop. All lepton lines are directed, and two external photon lines are distinguished.

The algorithm is as follows:

(1) A vertex to which an external photon line labeled by "s" is attached is chosen as the first element of the sequence. Assign the index "0" to this vertex, and assign numeric indices to other vertices sequentially along the loop in a certain direction.
(2) Another vertex is chosen to which the other external photon line labeled by "t" is attached. There are $(2n-1)$ choices of vertices.
(3) The remaining $(2n-2)$ vertices are made into $(n-1)$ pairs. Each pair corresponds to an internal photon line that connects the two vertices of that pair. There are $(2n-3)!!$ ways to construct $(n-1)$ pairs.

Therefore, the total number of diagrams is $(2n-1)\times(2n-3)!!$.

Taking into account the time-reversal symmetry of QED and the symmetry by the permutation of Lorentz indices of external photon lines, we identify the equivalent diagrams with respect to the reversal of sequences and exchange of symbols "s" and "t." In this fashion we obtain a complete set of topologically distinct diagrams with an appropriate weight factor of the symmetry. In the case of the Set I (i) we have 39 distinct diagrams, which are shown in Fig. 3.

C. Photon self-energy amplitude

The momentum representation of the $2n$th-order vacuum-polarization diagram G has the form given by the Feynman-Dyson rule:

$$i\Pi_G^{\mu\nu}(q) = (-1)(-ie)^{2n}\int\frac{d^4l_1}{(2\pi)^4}\cdots\frac{d^4l_n}{(2\pi)^4} \times \mathrm{Tr}\left[\gamma^\mu\frac{i}{\not p_1 - m}\gamma^a\cdots\gamma^\nu\frac{i}{\not p_{i+1}-m}\gamma_a\cdots\right]\prod_j\left(\frac{-i}{k_j^2}\right), \quad (7)$$

where m is the rest mass of loop leptons, p_i is the momentum flowing on the lepton line i, and k_j is the momentum flowing on the photon line j. These momenta are given as linear combinations of the loop momenta $l_1, \ldots, l_n$, and the external momentum q.

As a convention, the flow of the external momentum q is chosen as shown in Fig. 4, where each fraction $q/2$ flows on the upper (lower) semicircle that consists of lepton lines $1, \ldots, i$ $(i+1, \ldots, 2n)$, respectively. The function (7) is quadratically divergent, and we assume that the above expression is appropriately regularized by the Pauli-Villars regularization.

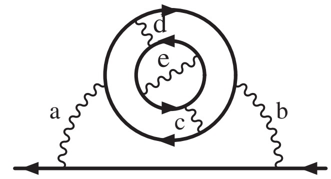

FIG. 2. ab(acbd)(cede): An example of the sequential representation of a diagram of Set I(g).

[1]This convention may still have ambiguities. However, it works for the diagrams with a single lepton loop that are discussed in the present article.

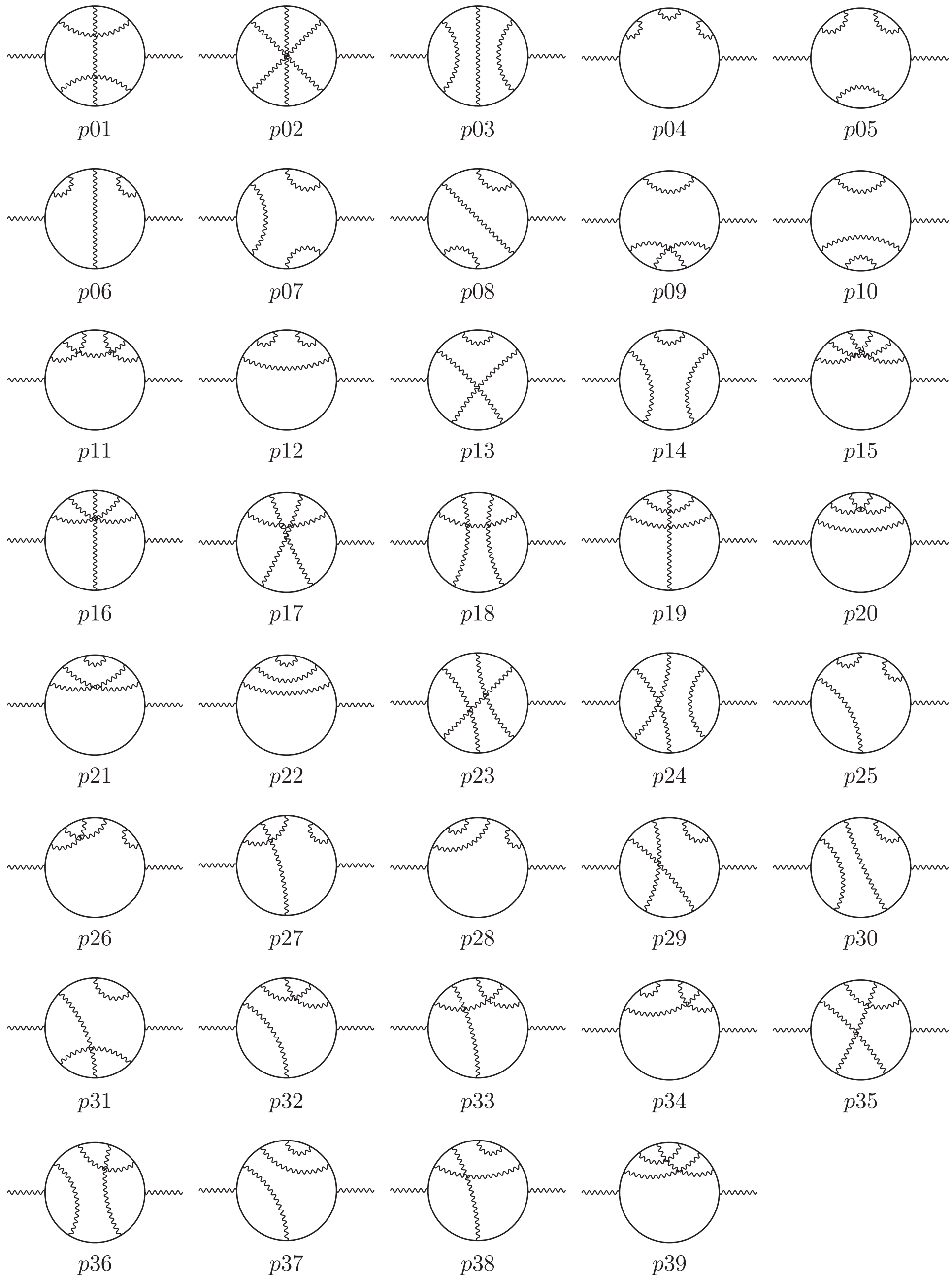

FIG. 3. Eighth-order vacuum-polarization diagrams containing one closed lepton loop.

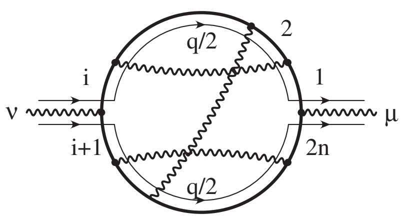

FIG. 4. Flow of extra momentum q.

We adopt here an approach that exploits gauge invariance of the sum $\Pi^{\mu\nu} = \sum_G \Pi_G^{\mu\nu}$ which allows us to ignore the gauge-dependent part of (7). The gauge invariance ensures the identity

$$q_\alpha \Pi^{\alpha\nu}(q) = 0, \tag{8}$$

which holds for Pauli-Villars regularized function $\Pi^{\mu\nu}$. Differentiating it with respect to q_μ, we obtain

$$\Pi^{\mu\nu}(q) = -q_\alpha \frac{\partial \Pi^{\alpha\nu}}{\partial q_\mu}. \tag{9}$$

Since q_μ is the external momentum, the order of q_μ and the integration over the loop momenta can be interchanged, as far as the integral is properly regularized. Thus we can write

$$i\Pi_G^{\mu\nu}(q) = -(-1)(-ie)^{2n} q_\alpha \int \frac{d^4 l_1}{(2\pi)^4} \cdots \frac{d^4 l_n}{(2\pi)^4} \frac{\partial}{\partial q_\mu} \mathrm{Tr}\left[\gamma^\alpha \frac{i}{\not p_1 - m} \cdots \gamma^\nu \frac{i}{\not p_{i+1} - m} \cdots\right] \prod_j \left(\frac{-i}{k_j^2}\right)\Bigg|_{\mathrm{PV}}. \tag{10}$$

Carrying out the differentiation with respect to q_μ, we obtain

$$i\Pi_G^{\mu\nu}(q) = -(-1)(-ie)^{2n} i^{2n} \int \frac{d^4 l_1}{(2\pi)^4} \cdots \frac{d^4 l_n}{(2\pi)^4} \sum_j \mathrm{Tr}\left[\not q \frac{1}{\not p_1 - m} \cdots \left\{\frac{1}{\not p_j - m}\left(\mp \frac{\gamma^\mu}{2}\right) \frac{1}{\not p_j - m}\right\} \cdots \gamma^\nu \frac{1}{\not p_{i+1} - m} \cdots\right] \times \prod_j \left(\frac{-i}{k_j^2}\right)\Bigg|_{\mathrm{PV}}, \tag{11}$$

where the minus (plus) sign in ($\mp \gamma^\mu/2$) is taken when the line j belongs to the upper (lower) semicircle of the diagram.

The calculation can be simplified using the identity [25]

$$\frac{(\not p_i + m_i)\gamma^\mu(\not p_i + m_i)}{(p_i^2 - m_i^2)^2} = 2D_i^\mu(\not D_i + m_i)\frac{1}{(p_i^2 - m_i^2)^2}, \tag{12}$$

where D_i^μ is defined by

$$D_i^\mu = \frac{1}{2}\int_{m_i^2}^\infty dm_i^2 \frac{\partial}{\partial q_{i\mu}}. \tag{13}$$

We can now move the trace operation outside the k integration. With the help of Feynman parameters z_i associated with the line i, the denominators can be combined into one, and then the momentum integration can be carried out analytically. Now we bring back D operators inside the z integral and obtain

$$\Pi^{\mu\nu}(q) = -\left(-\frac{\alpha}{4\pi}\right)^n \int \frac{(dz)}{U^2}\left(\sum_j \mp z_j D_j^\mu\right) \times \mathrm{Tr}[\not q(\not D_i + m) \cdots \gamma^\nu \cdots]\frac{1}{V^n}, \tag{14}$$

where

$$(dz) \equiv \delta\left(1 - \sum_i z_i\right)\prod_i dz_i, \qquad i = 1, 2, \ldots, 3n-1. \tag{15}$$

U is a homogeneous function of z's determined from the topology of the diagram and V is defined by

$$V = V_0 - q^2 G, \qquad V_0 = \sum_{\text{all lepton lines}} z_i m^2, \qquad G = \sum_{i\in\mathcal{P}(\mu,\nu)} z_i A_i, \tag{16}$$

where the path $\mathcal{P}(\mu, \nu)$ is arbitrarily taken to run between two external photon lines. In the present case, we choose the convention that the path $\mathcal{P}$ runs on the upper half part of the loop of diagrams shown in Fig. 4.

From Lorentz invariance and gauge invariance we have the general structure

$$\Pi_{G\mu\nu}^{(2n)}(q) = (q_\mu q_\nu - q^2 g_{\mu\nu})\tilde\Pi_G^{(2n)}(q^2) + (\text{gauge-dependent terms}). \tag{17}$$

The Lorentz scalar $\tilde\Pi^{(2n)}$ has only a logarithmic divergence so that the number of auxiliary masses in Pauli-Villars regularization can be reduced to one. The renormalizations of subdiagram UV divergences are carried out independently of each other. Gauge-dependent terms cancel out when all diagrams of Set I(i) are combined. The charge renormalization can be achieved by

$$\Pi_G^{(2n)}(q^2) = \tilde\Pi_G^{(2n)}(q^2) - \tilde\Pi_G^{(2n)}(0). \tag{18}$$

For the case $n = 4$, which is our concern, $\tilde\Pi_G^{(2n)}(q^2)$ can be expressed in the form

$$\tilde\Pi_G^{(8)}(q^2) = \int (dz)\left[\frac{D_0 + q^2 B_0 + q^4 C_0 + q^6 E_0}{U^2 V^3} + \frac{D_1 + q^2 B_1 + q^4 C_1}{U^3 V^2} + \frac{D_2 + q^2 B_2}{U^4 V} + \frac{D_3}{U^5}\ln\left[\frac{V_0}{V}\right]\right], \tag{19}$$

when the D operation is carried out [omitting the factor $(\alpha/\pi)^4$ for simplicity]. The coefficients D_l, B_l, C_l, and E_l are functions of building blocks B_{ij} and A_j described in the following subsection. The suffix l labels the number of contractions of D operators.

D. Building blocks

Building blocks U and B_{ij} are homogeneous polynomials of degree n and $n-1$ of the Feynman parameters z_i, respectively. They are determined by the topological structure of the diagram called the chain diagram that is derived by amputating all external lines and disregarding distinction of the types of lines [25].

The fundamental set of circuits of the chain diagram that consists of n independent self-nonintersecting closed loops is chosen in the following manner. One type of circuit is formed by an internal photon line and consecutive lepton lines that connect the endpoints of the photon line. The direction of the circuit is chosen to be that of the lepton lines. We may assign the direction of the photon line accordingly. There are $n-1$ circuits of this sort. The nth circuit is chosen to be the closed lepton loop itself.

Then, for i and j that label the lines of the chain diagram, U and B_{ij} are given by

$$U_{st} = \sum_k z_k \xi_{k,s}\xi_{k,t}, \qquad U = \det_{st} U_{st},$$
$$B_{ij} = U\sum_{s,t}\xi_{i,s}\xi_{j,t}(U^{-1})_{st}, \tag{20}$$

where s and t refer to the circuits. The loop matrix $\xi_{k,c}$ takes (1, -1, 0) according to whether the line i is (along, against, outside of) the circuit c.

Once U and B_{ij} are obtained, another building block, the scalar current A_j, is given by

$$A_j = \sum_{i\in\mathcal{P}(\mu,\nu)} (\delta_{ij} - z_i B_{ij}/U). \tag{21}$$

E. UV divergence

The amplitude constructed thus far may have UV divergences when the sum of Feynman parameters of one or more internal loops tends to zero. We adopt subtractive renormalization here in a suitable way for numerical treatment. The subtraction terms are prepared as an integral over the same Feynman parameter space as the original unrenormalized amplitude so that the divergences of the amplitude are canceled pointwise. These subtraction terms are constructed by a simple algorithm called the K operation [25] for each occurrence of subdiagram UV divergences. The whole divergent structure of a diagram is recognized by Zimmermann's forest formula.

The subdiagrams relevant for the UV divergence are of the self-energy type or vertex type. For the proper lepton loops of the present concern, such a subdiagram is represented by an open segment of the lepton loop, which involves vertices and lepton lines in the segment, and photon lines whose endpoints are included in the segment. Therefore, we have to examine every segment of the lepton loop whenever it corresponds to a one-particle irreducible subdiagram of self-energy type or vertex type.

The inclusion relation of subdiagrams are found by examining the inclusion relation of the segments: they are *independent* or *overlapping*, or one segment is completely *included* in the other. Once the relation is known, the complete set of forests are constructed by finding all possible sets of subdiagrams whose elements are not overlapping with each other.

Each forest corresponds to a particular emergence of UV divergence, and it is related to a subtraction term in the subtractive renormalization. For a vertex subdiagram $\mathcal{S}$ of a diagram $\mathcal{G}$, the subtraction term defined by the K operation factorizes analytically by construction as

$$L_{\mathcal{S}}^{\rm UV}\Pi_{\mathcal{G}/\mathcal{S}}, \tag{22}$$

where $L_{\mathcal{S}}^{\rm UV}$ is the UV-divergent part of the vertex renormalization constant for the subdiagram S, and $\Pi_{\mathcal{G}/\mathcal{S}}$ is the amplitude of the reduced diagram $\mathcal{G}/\mathcal{S}$. When a subdiagram $\mathcal{S}$ is of the self-energy type, the subtraction term factorizes analytically as

$$\delta m_{\mathcal{S}}^{\rm UV}\Pi_{\mathcal{G}/\mathcal{S}(i^*)} + B_{\mathcal{S}}^{\rm UV}\Pi_{\mathcal{G}/\mathcal{S},i'}, \tag{23}$$

where $\delta m_{\mathcal{S}}^{\rm UV}$ is the UV-divergent part of the mass renormalization constant $\delta m_{\mathcal{S}}$, and $B_{\mathcal{S}}^{\rm UV}$ is the UV-divergent part of the wave-function renormalization constant $B_{\mathcal{S}}$. When a forest consists of more than one subdiagram, the subtraction term becomes products of renormalization constants and reduced amplitudes.

III. INSERTION OF $\Pi^{(8)}$ IN M_2

The easiest way to insert the eighth-order vacuum-polarization loops in M_2 is by the formula [29,30]

$$M_{2,P_8} = -\int_0^1 dy(1-y)\Pi^{(8)}\left(\frac{-y^2}{1-y}\right), \tag{24}$$

where $\Pi^{(8)}$ is given by Eqs. (18) and (19). It is straightforward to include this in the automated code generation system.

As a check of the integration codes, we have also derived the following formula from Eq. (19) applying the method described in Ref. [25] which yields

$$\begin{aligned} M_{2,P_8} = \int_0^1 dy(1-y)\int(dz)\Big[&\frac{D_0}{U^2V_0^3W^3}(W^3-(W-1)^3) \\ &+\frac{B_0}{U^2GV_0^2W^3}(W-1)^2 - \frac{C_0}{U^2G^2V_0W^3}(W-1) \\ &+\frac{E_0}{U^2G^3W^3} + \frac{D_1}{U^3V_0^2W^2}(W^2-(W-1)^2) \\ &+\frac{B_1}{U^3GV_0W^2}(W-1) - \frac{C_1}{U^3G^2W^2} + \frac{D_2}{U^4V_0W} \\ &+\frac{B_2}{U^4GW} + \frac{D_3}{U^5}\ln\left(\frac{W}{W-1}\right)\Big], \end{aligned} \tag{25}$$

where

$$W = 1 + \frac{V_0}{G}\frac{1-y}{y^2}. \tag{26}$$

The UV-divergent terms of M_{2,P_8} can be isolated by the K operation. See Appendix C for details.

IV. RESIDUAL RENORMALIZATION

The standard on-the-mass-shell renormalization of our vacuum-polarization function $\Pi^{(8)}$ is given explicitly in Appendix B. Actually, it is not suitable for evaluation of these terms on the computer, because individual terms of these functions are UV divergent. Thus it is necessary to convert them into sums of UV-finite quantities. This is achieved by an intermediate renormalization procedure carried out by the K operation shown in Appendix C. The K operation subtracts only the UV-divergent parts of renormalization constants. In order to obtain the standard on-the-mass-shell renormalization, the remaining UV-finite terms must be removed by a procedure called residual renormalization.

Substituting expressions given in Appendix C into corresponding expressions in Appendix B, and making use of various subdiagram relations listed in Appendix D, we can convert the right-hand side of equations of Appendix B into the sum of finite quantities. Collecting all terms thus created we obtain

$$\begin{aligned} a_{l_1}^{(10)}[\mathrm{I(i)}^{(l_1 l_2)}] &= M_{2,\Delta P_8}^{(l_1 l_2)} - 6\Delta LB_2 M_{2,\Delta P_6}^{(l_1 l_2)} + \{14(\Delta LB_2)^2 - 4\Delta LB_4\} M_{2,\Delta P_4}^{(l_1 l_2)} \\ &+ \{-14(\Delta LB_2)^3 + 14\Delta LB_4 \Delta LB_2 - 2\Delta LB_6\} M_{2,P_2}^{(l_1 l_2)} \\ &- \Delta\delta m_4 M_{2,\Delta P_4^*}^{(l_1 l_2)} + (12\Delta LB_2 \Delta\delta m_4 + 2\Delta\delta m_4 \Delta\delta m_2^* - 2\Delta\delta m_6) M_{2,P_{2^*}}^{(l_1 l_2)}. \end{aligned} \tag{27}$$

Suppressing the superscript $(l_1 l_2)$ for simplicity the residual renormalizaton terms are defined as follows:

$$\begin{aligned} M_{2,\Delta P_8} &= \sum_{i=p01}^{p39} n_{Fi} M_{2,i}, \\ M_{2,\Delta P_6} &= \sum_{\beta=A}^{H} \eta_\beta M_{2,P_{6\beta}}, \\ M_{2,\Delta P_4} &= M_{2,P_{4a}} + 2M_{2,P_{4b}}, \\ M_{2,\Delta P_{4^*}} &= M_{2,P_{4a^*}} + 2M_{2,P_{4b^*}}, \\ \Delta LB_6 &= \sum_{\beta=A}^{H} \lambda_\beta \Delta LB_{6\beta}, \\ \Delta LB_4 &= \sum_{i=1}^{3} (\Delta L_{4a,i} + \Delta L_{4b,i}) + \Delta B_{4a} + \Delta B_{4b}, \\ \Delta LB_2 &= \Delta B_2 \\ \Delta\delta m_6 &= \sum_{\beta=A}^{H} \lambda_\beta \Delta\delta m_{6\beta}, \\ \Delta\delta m_4 &= \Delta\delta m_{4a} + \Delta\delta m_{4b}, \end{aligned} \tag{28}$$

where $n_{Fi} = 1$ for $i = p01, p02, p03$, $n_{Fi} = 2$ for $i = p04, \ldots, p22$, and $n_{Fi} = 4$ for $i = p23, \ldots, p39$, $\eta_A = \eta_C = \eta_D = \eta_F = 2$, $\eta_B = \eta_G = \eta_H = 1$, $\eta_E = 4$, and $\lambda_A = \lambda_B = \lambda_C = \lambda_E = \lambda_F = \lambda_H = 1$, $\lambda_D = \lambda_G = 2$. $\Delta LB_{6\beta}$, $\beta = A, \ldots, H$, are defined in Appendix D. Numerical values of ΔLB_2, $\Delta\delta m_6$, $\Delta\delta m_4$, $M_{2,P_{2^*}}$, δm_{2^*}, etc., are listed in Table II.

The coefficient -6 of $M_{2,\Delta P_6}$ in (27) can be readily understood noting that the vacuum-polarization function Π_6 has 6 fermion lines into which a two-point vertex can be inserted. This insertion is the source of the wave-function renormalization constant B_2 and the self-mass δm_2 term. Since $\Delta\delta m_2 = 0$, however, only the ΔB_2 survives in (27). For convenience let us call this an insertion of B_2.

We find 14 different ways of insertion of two B_2's in Π_4. Ten come from insertions of two disconnected second-order self-energy diagrams and four come from insertions of the fourth-order self-energy diagram in which a second-order self-energy diagram is completely included in another second-order self-energy diagram. Three B_2's can be inserted in Π_2 in 14 ways. Insertion of one B_4 and one B_2 in Π_2 can also be made in 14 different ways. All three of these terms should be accompanied by terms proportional to $\Delta\delta m_2$ which, however, vanish in our formulation based on the K operation.

The factor -4 in $-4\Delta LB_4 M_{2,\Delta P_4}$ is due to the fact that Π_4 has 4 fermion lines into which B_4 can be inserted. The apparent absence of the coefficient 4 in $-\Delta\delta m_4 M_{2,\Delta P_{4^*}}$ can be accounted for by the fact that Π_4 has four fermion lines into which a two-point vertex can be inserted. Thus the coefficient 4 is absorbed in the definition of Π_{4^*}. This term is present in (27) since $\Delta\delta m_4$ is nonvanishing.

Finally one B_6 can be inserted in Π_2 in two ways. The factor 2 in $-2\Delta\delta m_6 M_{2,P_{2^*}}$ is the same as that of $-2\Delta B_6 M_{2,P_2}$. The term $2\Delta\delta m_4 \Delta\delta m_{2^*} M_{2,P_{2^*}}$ is related to the subdiagram of $-2\Delta\delta m_6 M_{2,P_{2^*}}$ except for the factor -1. Application of the K operation on the second-order self-energy subdiagram of Π_{4^*} yields $6\Delta B_2 \Pi_{2^*}$. Application of the K operation on the second-order self-energy subdiagram of δm_6 yields 6 $\Delta\delta m_4 \Delta B_2$. Together they give $12\Delta LB_2 \Delta\delta m_4 M_{2,P_{2^*}}$.

A similar argument can be given starting from vertex renormalization subdiagrams, although it does not give information on the $\Delta\delta m$ term. Consideration of vertex renormalization is not necessary, however, since $a_{l_1}^{(10)}[\mathrm{I(i)}]$ is free from infrared (IR) divergence so that L_n is always combined with B_n to form an finite combination ΔLB_n.

The reason the coefficients of residual renormalization terms can be determined by the argument described above is that the UV-finite parts are not affected by the K operation which deals only with UV-divergent parts so that the coefficients of residual renormalization terms inherit the structure of the standard renormalization unaltered.

V. NUMERICAL EVALUATION OF $M_{2,P_8}^{(ee)}$

FORTRAN codes of our diagrams are generated by GENCODEVPN following the procedures described in Sec. II. The validity of GENCODEVPN has been tested thoroughly for diagrams of Set II(d) whose integrals are known by several other means [31–34]. Numerical integration was carried out by an adaptive-iterative Monte Carlo numerical integration routine VEGAS [35] with 10^8 sampling points per iteration and 150 iterations followed by 10^9 sampling points per iteration and 10 iterations. The results are summarized in Tables I and II. From these data we obtain

$$a_e^{(10)}[\mathrm{I(i)}^{(ee)}] = 0.017\,47\,(11). \tag{29}$$

TABLE I. Contributions of diagrams of Set I(i) to a_e for $(l_1 l_2) = (ee)$. The superscript (ee) is suppressed for simplicity. The multiplicity n_F is the number of vertex diagrams represented by the integral and is incorporated in the numerical value. All integrals are evaluated initially with 10^8 sampling points per iteration, iterated 150 times, followed by 10^9 points, iterated 10 times.

Integral	n_F	Value (Error) including n_F	Sampling per iteration	Number of iterations
$M_{2,p01}$	1	0.035 760 8 (60)	1×10^8, 1×10^9	150, 10
$M_{2,p02}$	1	0.017 303 9 (40)	1×10^8, 1×10^9	150, 10
$M_{2,p03}$	1	0.039 757 3 (73)	1×10^8, 1×10^9	150, 10
$M_{2,p04}$	2	0.037 755 2 (93)	1×10^8, 1×10^9	150, 10
$M_{2,p05}$	2	0.062 796 0 (190)	1×10^8, 1×10^9	150, 10
$M_{2,p06}$	2	0.129 748 0 (225)	1×10^8, 1×10^9	150, 10
$M_{2,p07}$	2	0.128 655 4 (251)	1×10^8, 1×10^9	150, 10
$M_{2,p08}$	2	0.103 304 6 (167)	1×10^8, 1×10^9	150, 10
$M_{2,p09}$	2	−0.038 968 7 (92)	1×10^8, 1×10^9	150, 10
$M_{2,p10}$	2	−0.057 281 7 (105)	1×10^8, 1×10^9	150, 10
$M_{2,p11}$	2	0.020 893 9 (34)	1×10^8, 1×10^9	150, 10
$M_{2,p12}$	2	0.038 800 8 (54)	1×10^8, 1×10^9	150, 10
$M_{2,p13}$	2	0.017 581 6 (166)	1×10^8, 1×10^9	150, 10
$M_{2,p14}$	2	0.090 813 8 (165)	1×10^8, 1×10^9	150, 10
$M_{2,p15}$	2	0.008 522 3 (17)	1×10^8, 1×10^9	150, 10
$M_{2,p16}$	2	0.023 211 8 (28)	1×10^8, 1×10^9	150, 10
$M_{2,p17}$	2	−0.009 190 1 (34)	1×10^8, 1×10^9	150, 10
$M_{2,p18}$	2	0.011 705 8 (31)	1×10^8, 1×10^9	150, 10
$M_{2,p19}$	2	0.024 548 0 (48)	1×10^8, 1×10^9	150, 10
$M_{2,p20}$	2	0.028 129 1 (24)	1×10^8, 1×10^9	150, 10
$M_{2,p21}$	2	−0.014 422 7 (29)	1×10^8, 1×10^9	150, 10
$M_{2,p22}$	2	0.012 984 7 (39)	1×10^8, 1×10^9	150, 10
$M_{2,p23}$	4	0.008 650 4 (35)	1×10^8, 1×10^9	150, 10
$M_{2,p24}$	4	0.037 873 8 (95)	1×10^8, 1×10^9	150, 10
$M_{2,p25}$	4	0.168 761 3 (302)	1×10^8, 1×10^9	150, 10
$M_{2,p26}$	4	−0.061 567 5 (141)	1×10^8, 1×10^9	150, 10
$M_{2,p27}$	4	−0.145 657 6 (325)	1×10^8, 1×10^9	150, 10
$M_{2,p28}$	4	−0.078 819 8 (148)	1×10^8, 1×10^9	150, 10
$M_{2,p29}$	4	0.110 765 8 (297)	1×10^8, 1×10^9	150, 10
$M_{2,p30}$	4	0.217 591 7 (407)	1×10^8, 1×10^9	150, 10
$M_{2,p31}$	4	−0.149 396 6 (349)	1×10^8, 1×10^9	150, 10
$M_{2,p32}$	4	−0.122 439 0 (139)	1×10^8, 1×10^9	150, 10
$M_{2,p33}$	4	0.043 600 9 (107)	1×10^8, 1×10^9	150, 10
$M_{2,p34}$	4	−0.003 177 4 (75)	1×10^8, 1×10^9	150, 10
$M_{2,p35}$	4	−0.054 641 9 (129)	1×10^8, 1×10^9	150, 10
$M_{2,p36}$	4	−0.138 680 8 (150)	1×10^8, 1×10^9	150, 10
$M_{2,p37}$	4	−0.102 260 8 (164)	1×10^8, 1×10^9	150, 10
$M_{2,p38}$	4	−0.060 892 7 (234)	1×10^8, 1×10^9	150, 10
$M_{2,p39}$	4	−0.008 689 5 (43)	1×10^8, 1×10^9	150, 10

TABLE II. Auxiliary integrals for Set I(i). Some integrals are known exactly. Other integrals are obtained by the integration routine VEGAS. The superscript $(l_1 l_2)$, where $l_i = e, m, t$, indicates that the open and closed fermion lines consist of fermions l_1 and l_2, respectively. The letters e, m, and t stand for electron, muon, and tau-lepton, respectively.

Integral	Value (Error)	Integral	Value (Error)
$\Delta\delta m_2^*$	−0.75	ΔLB_2	0.75
$\Delta\delta m_4$	1.906 340 (21)	ΔLB_4	0.027 930 (28)
$\Delta\delta m_6$	−2.340 65 (48)	ΔLB_6	0.100 86 (77)
$M_{2,P2}^{(ee)}$	0.015 687 421 ...	$M_{2,P2}^{(em)}$	$0.519\,762\,(21) \times 10^{-6}$
$M_{2,P2}^{(me)}$	1.094 258 28 ...	$M_{2,P2}^{(mt)}$	0.000 078 067 (4)
$M_{2,P2^*}^{(ee)}$	−0.012 702 383 ...	$M_{2,P2^*}^{(em)}$	$-0.519\,719\,(17) \times 10^{-6}$
$M_{2,P2^*}^{(me)}$	−0.161 084 05 ...	$M_{2,P2^*}^{(mt)}$	−0.000 077 655 (3)
$M_{2,\Delta P4}^{(ee)}$	0.076 401 785 ...	$M_{2,\Delta P4}^{(em)}$	$0.275\,271\,(1) \times 10^{-5}$
$M_{2,\Delta P4}^{(me)}$	3.135 059 01 (2)	$M_{2,\Delta P4}^{(mt)}$	0.000 412 61 (3)
$M_{2,\Delta P4^*}^{(ee)}$	−0.117 770 (12)	$M_{2,\Delta P4^*}^{(em)}$	−0.000 005 505 (1)
$M_{2,\Delta P4^*}^{(me)}$	−0.754 40 (13)	$M_{2,\Delta P4^*}^{(mt)}$	−0.000 819 49 (8)
$M_{2,\Delta P6}^{(ee)}$	0.187 046 (7)	$M_{2,\Delta P6}^{(em)}$	$0.731\,632\,(71) \times 10^{-5}$
$M_{2,\Delta P6}^{(me)}$	5.543 94 (42)	$M_{2,\Delta P6}^{(mt)}$	0.001 094 28 (7)

VI. NUMERICAL EVALUATION OF $M_{2,P_8}^{(em)}$

Once FORTRAN programs for mass-independent diagrams are obtained, it is straightforward to evaluate the contribution of the mass-dependent term $A_2^{(10)}(m_e/m_\mu)$. We simply have to choose an appropriate loop fermion mass. The results are summarized in Table III. From this table we obtain

$$a_e^{(10)}[\mathrm{I(i)}^{(em)}] = 0.000\,001\,666\,(24). \qquad (30)$$

The numerical data used to obtain (30) are listed in Tables II and III. The contribution $A_2^{(10)}(m_e/m_\tau)$ is 2 orders of magnitude smaller than (30) so that it is negligible at present.

VII. CONTRIBUTION TO THE MUON $g-2$

The codes described above can also be applied to calculate the contribution of the Set I(i) to the muon $g-2$. From Tables II and IV, we obtain

$$a_\mu^{(10)}[\mathrm{I(i)}^{(me)}] = 0.087\,1\,(59). \qquad (31)$$

We have also evaluated the tau-lepton contribution. The values listed in Tables II and V lead to

$$a_\mu^{(10)}[\mathrm{I(i)}^{(mt)}] = 0.000\,237\,(1). \qquad (32)$$

The contribution of Set I(i) diagrams to the muon $g-2$ was first discussed in Eq. (19) of Ref. [26] in which the renormalization group was efficiently used to pick up the leading logarithmic contribution:

$$a_\mu^{(10)}[\mathrm{I(i)}^{(me)}] = -\frac{1}{2}a_4^{[1]} + \frac{115}{512} - \frac{23}{128}\ln\left(\frac{m_\mu}{m_e}\right) + O(m_e/m_\mu), \qquad (33)$$

where $a_4^{[1]}$ is the constant term of the asymptotic expansion of the proper vacuum-polarization function $\Pi^{(8)}(q)$ of the eighth order, which was left undetermined. This constant can be determined from our numerical result Eq. (31):

$$a_4^{[1]}[\text{numerical}] = -1.641\,0\,(59). \qquad (34)$$

Recently the asymptotic analytic form of $a_4^{[1]}$ was obtained directly together with other eighth-order vacuum-polarization diagrams [28]. The explicit form of $a_4^{[1]}$ was given only in the slide of the conference talk [27], and reads

$$a_4^{[1]}[\text{anal.-asympt.}] = -1.971\,6 + O(m_e/m_\mu). \qquad (35)$$

Substituting this value into Eq. (33), Chetyrkin obtained the asymptotic contribution of the Set I(i)

$$a_\mu^{(10)}[\text{I(i): anal.-asympt.}] = 0.252\,37 + O(m_e/m_\mu). \qquad (36)$$

Whether this is in agreement with our result (31) or not is somewhat subtle and will be discussed in the next section.

VIII. SUMMARY

In this paper we obtained the eighth-order vacuum-polarization function $\Pi^{(8)}(q^2)$ as a sum of Feynman-parametric integrals. It is then applied to the calculation

TABLE III. Contributions of diagrams of Set I(i) to a_e for $(l_1 l_2) = (em)$. The multiplicity n_F is the number of vertex diagrams represented by the integral and is incorporated in the numerical value. The superscript (em) is omitted for simplicity. All integrals are evaluated in double precision.

Integral	n_F	Value (Error) including n_F	Sampling per iteration	Number of iterations
$M_{2,p01}$	1	$0.115\,63\,(3) \times 10^{-5}$	1×10^8	50
$M_{2,p02}$	1	$0.077\,01\,(3) \times 10^{-5}$	1×10^8	50
$M_{2,p03}$	1	$0.201\,24\,(5) \times 10^{-5}$	1×10^8	50
$M_{2,p04}$	2	$0.147\,75\,(6) \times 10^{-5}$	1×10^8	50
$M_{2,p05}$	2	$0.236\,81\,(14) \times 10^{-5}$	1×10^8	50
$M_{2,p06}$	2	$0.484\,29\,(16) \times 10^{-5}$	1×10^8	50
$M_{2,p07}$	2	$0.488\,27\,(19) \times 10^{-5}$	1×10^8	50
$M_{2,p08}$	2	$0.400\,43\,(12) \times 10^{-5}$	1×10^8	50
$M_{2,p09}$	2	$-0.148\,04\,(6) \times 10^{-5}$	1×10^8	50
$M_{2,p10}$	2	$-0.248\,34\,(8) \times 10^{-5}$	1×10^8	50
$M_{2,p11}$	2	$0.071\,31\,(2) \times 10^{-5}$	1×10^8	50
$M_{2,p12}$	2	$0.168\,94\,(4) \times 10^{-5}$	1×10^8	50
$M_{2,p13}$	2	$0.052\,85\,(12) \times 10^{-5}$	1×10^8	50
$M_{2,p14}$	2	$0.409\,41\,(12) \times 10^{-5}$	1×10^8	50
$M_{2,p15}$	2	$0.043\,04\,(1) \times 10^{-5}$	1×10^8	50
$M_{2,p16}$	2	$0.064\,53\,(1) \times 10^{-5}$	1×10^8	50
$M_{2,p17}$	2	$-0.044\,76\,(2) \times 10^{-5}$	1×10^8	50
$M_{2,p18}$	2	$0.037\,80\,(2) \times 10^{-5}$	1×10^8	50
$M_{2,p19}$	2	$0.088\,50\,(3) \times 10^{-5}$	1×10^8	50
$M_{2,p20}$	2	$0.114\,22\,(1) \times 10^{-5}$	1×10^8	50
$M_{2,p21}$	2	$-0.062\,59\,(2) \times 10^{-5}$	1×10^8	50
$M_{2,p22}$	2	$0.047\,81\,(2) \times 10^{-5}$	1×10^8	50
$M_{2,p23}$	4	$0.034\,72\,(2) \times 10^{-5}$	1×10^8	50
$M_{2,p24}$	4	$0.148\,88\,(7) \times 10^{-5}$	1×10^8	50
$M_{2,p25}$	4	$0.652\,31\,(23) \times 10^{-5}$	1×10^8	50
$M_{2,p26}$	4	$-0.235\,83\,(10) \times 10^{-5}$	1×10^8	50
$M_{2,p27}$	4	$-0.491\,34\,(21) \times 10^{-5}$	1×10^8	50
$M_{2,p28}$	4	$-0.347\,15\,(11) \times 10^{-5}$	1×10^8	50
$M_{2,p29}$	4	$0.389\,88\,(21) \times 10^{-5}$	1×10^8	50
$M_{2,p30}$	4	$0.944\,16\,(33) \times 10^{-5}$	1×10^8	50
$M_{2,p31}$	4	$-0.512\,63\,(25) \times 10^{-5}$	1×10^8	50
$M_{2,p32}$	4	$-0.477\,71\,(9) \times 10^{-5}$	1×10^8	50
$M_{2,p33}$	4	$0.146\,82\,(6) \times 10^{-5}$	1×10^8	50
$M_{2,p34}$	4	$-0.000\,10\,(5) \times 10^{-5}$	1×10^8	50
$M_{2,p35}$	4	$-0.171\,64\,(9) \times 10^{-5}$	1×10^8	50
$M_{2,p36}$	4	$-0.548\,36\,(11) \times 10^{-5}$	1×10^8	50
$M_{2,p37}$	4	$-0.498\,39\,(13) \times 10^{-5}$	1×10^8	50
$M_{2,p38}$	4	$-0.179\,07\,(15) \times 10^{-5}$	1×10^8	50
$M_{2,p39}$	4	$-0.044\,15\,(3) \times 10^{-5}$	1×10^8	50

of the tenth-order lepton $g-2$. Collecting (29) and (30) we obtain the contribution of the gauge-invariant Set I(i) to the electron $g-2$:

$$a_e^{(10)}[\mathrm{I(i)}^{(\mathrm{all})}] = 0.017\,47\,(11). \tag{37}$$

From (29), (31), and (32) we obtain the contribution from Set I(i) to the muon $g-2$:

$$a_\mu^{(10)}[\mathrm{I(i)}^{(\mathrm{all})}] = 0.104\,8\,(59). \tag{38}$$

It is difficult to decide whether our result (31) and asymptotic result (36) are in agreement or not. In order to illuminate this problem it may be helpful to compare a_μ of similar structure in lower orders.

The sixth-order a_μ obtained by inserting a proper fourth-order vacuum-polarization $\Pi^{(4)}$ in the second order M_2 gives [18,36]

$$\begin{aligned} a_\mu^{(6)}[\mathrm{num.}] &= 1.493\,671\,581\,(8), \\ a_\mu^{(6)}[\mathrm{asym.}] &= 1.5173 + O(m_e/m_\mu), \end{aligned} \tag{39}$$

where the overall factor $(\alpha/\pi)^3$ is omitted for simplicity.

The eighth-order a_μ obtained by inserting a proper sixth-order vacuum-polarization $\Pi^{(6)}$ in the second order M_2 gives the coefficients of $(\alpha/\pi)^4$:

$$\begin{aligned} a_\mu^{(8)}[\text{num.}] &= -0.230\,596\,(416), \\ a_\mu^{(8)}[\text{Padé}] &= -0.230\,362\,(5), \\ a_\mu^{(8)}[\text{asym.}] &= -0.290\,987 + O(m_e/m_\mu), \end{aligned} \tag{40}$$

where the numerical evaluation $a_\mu^{(8)}$[num.] is from [33,37], the Padé approximation $a_\mu^{(8)}$[Padé] is from [31], and the asymptotic result $a_\mu^{(8)}$[asym.] is from [38]. Note that the asymptotic result of (40) contains the leading logarithmic and next-to-leading constant terms.

The difference between the numerical and asymptotic results comes from the contribution of order m_e/m_μ. From the sixth-order (39), eighth-order (40), and tenth-order cases we find

TABLE IV. Contributions of diagrams of Set I(i) to a_μ for $(l_1 l_2) = (me)$. The multiplicity n_F is the number of vertex diagrams represented by the integral and is incorporated in the numerical value. The superscript (me) is omitted for simplicity. All integrals are evaluated initially with sampling points 10^8 per iteration, iterated 50 times, followed by 10^9 points per iteration, iterated 200 times, and 10^{10} points, iterated 10 to 80 times.

Integral	n_F	Value (Error) including n_F	Sampling per iteration	Number of iterations
$M_{2,p01}$	1	5.475 765 (50)	1×10^8, 1×10^9, 1×10^{10}	50, 200, 40
$M_{2,p02}$	1	−3.639 035 (13)	1×10^8, 1×10^9, 1×10^{10}	50, 200, 40
$M_{2,p03}$	1	1.014 582 (56)	1×10^8, 1×10^9, 1×10^{10}	50, 200, 40
$M_{2,p04}$	2	9.957 281 (77)	1×10^8, 1×10^9, 1×10^{10}	50, 200, 60
$M_{2,p05}$	2	11.130 636 (109)	1×10^8, 1×10^9, 1×10^{10}	50, 200, 80
$M_{2,p06}$	2	3.445 706 (95)	1×10^8, 1×10^9, 1×10^{10}	50, 200, 60
$M_{2,p07}$	2	1.150 328 (136)	1×10^8, 1×10^9, 1×10^{10}	50, 200, 70
$M_{2,p08}$	2	2.431 621 (98)	1×10^8, 1×10^9, 1×10^{10}	50, 200, 60
$M_{2,p09}$	2	−6.305 904 (87)	1×10^8, 1×10^9, 1×10^{10}	50, 200, 60
$M_{2,p10}$	2	3.576 267 (69)	1×10^8, 1×10^9, 1×10^{10}	50, 200, 10
$M_{2,p11}$	2	3.087 991 (41)	1×10^8, 1×10^9, 1×10^{10}	50, 200, 20
$M_{2,p12}$	2	2.681 026 (32)	1×10^8, 1×10^9, 1×10^{10}	50, 200, 10
$M_{2,p13}$	2	8.166 698 (70)	1×10^8, 1×10^9, 1×10^{10}	50, 200, 20
$M_{2,p14}$	2	−2.042 862 (97)	1×10^8, 1×10^9, 1×10^{10}	50, 200, 60
$M_{2,p15}$	2	−0.014 213 (9)	1×10^8, 1×10^9, 1×10^{10}	50, 200, 20
$M_{2,p16}$	2	3.556 341 (11)	1×10^8, 1×10^9, 1×10^{10}	50, 200, 20
$M_{2,p17}$	2	3.279 641 (8)	1×10^8, 1×10^9, 1×10^{10}	50, 200, 20
$M_{2,p18}$	2	−1.044 365 (5)	1×10^8, 1×10^9, 1×10^{10}	50, 200, 20
$M_{2,p19}$	2	3.238 053 (31)	1×10^8, 1×10^9, 1×10^{10}	50, 200, 20
$M_{2,p20}$	2	−0.804 464 (15)	1×10^8, 1×10^9, 1×10^{10}	50, 200, 20
$M_{2,p21}$	2	−2.002 941 (28)	1×10^8, 1×10^9, 1×10^{10}	50, 200, 20
$M_{2,p22}$	2	1.439 287 (14)	1×10^8, 1×10^9, 1×10^{10}	50, 200, 20
$M_{2,p23}$	4	2.246 387 (9)	1×10^8, 1×10^9, 1×10^{10}	50, 200, 20
$M_{2,p24}$	4	−1.943 020 (59)	1×10^8, 1×10^9, 1×10^{10}	50, 200, 50
$M_{2,p25}$	4	0.717 756 (211)	1×10^8, 1×10^9, 1×10^{10}	50, 200, 80
$M_{2,p26}$	4	−11.597 221 (131)	1×10^8, 1×10^9, 1×10^{10}	50, 200, 80
$M_{2,p27}$	4	−16.497 990 (188)	1×10^8, 1×10^9, 1×10^{10}	50, 200, 80
$M_{2,p28}$	4	7.463 932 (85)	1×10^8, 1×10^9, 1×10^{10}	50, 200, 60
$M_{2,p29}$	4	18.659 291 (133)	1×10^8, 1×10^9, 1×10^{10}	50, 200, 80
$M_{2,p30}$	4	−3.240 940 (198)	1×10^8, 1×10^9, 1×10^{10}	50, 200, 60
$M_{2,p31}$	4	−16.369 751 (181)	1×10^8, 1×10^9, 1×10^{10}	50, 200, 80
$M_{2,p32}$	4	−1.501 462 (99)	1×10^8, 1×10^9, 1×10^{10}	50, 200, 70
$M_{2,p33}$	4	8.005 147 (70)	1×10^8, 1×10^9, 1×10^{10}	50, 200, 20
$M_{2,p34}$	4	−5.994 355 (74)	1×10^8, 1×10^9, 1×10^{10}	50, 200, 60
$M_{2,p35}$	4	−13.319 800 (61)	1×10^8, 1×10^9, 1×10^{10}	50, 200, 20
$M_{2,p36}$	4	6.372 372 (64)	1×10^8, 1×10^9, 1×10^{10}	50, 200, 50
$M_{2,p37}$	4	−0.889 232 (94)	1×10^8, 1×10^9, 1×10^{10}	50, 200, 60
$M_{2,p38}$	4	−12.751 250 (97)	1×10^8, 1×10^9, 1×10^{10}	50, 200, 60
$M_{2,p39}$	4	1.541 038 (33)	1×10^8, 1×10^9, 1×10^{10}	50, 200, 20

$$\begin{aligned} a_\mu^{(6)}[\text{num.}] - a_\mu^{(6)}[\text{asym.}] &= -0.024, \\ a_\mu^{(8)}[\text{num.}] - a_\mu^{(8)}[\text{asym.}] &= 0.061, \\ a_\mu^{(10)}[\text{num.}] - a_\mu^{(10)}[\text{asym.}] &= 0.17. \end{aligned} \tag{41}$$

Note that the difference increases as the order of perturbation increases. Nevertheless, we cannot exclude the possibility that the difference between (31) and (36) is caused by some error. One possible cause is that the uncertainty of (31) is a gross underestimate because of insufficient data sampling. The situation might be similar to the case of $a_\mu^{(8)}$[num.] in early calculations [31,39,40] where poor sampling of integrands was found to be the cause of a large discrepancy with the Padé result. This problem was finally settled by going to a much larger sampling, which led to (40).

In order to examine the possibility of a gross underestimate of errors in (31), we evaluated the integrals with the sampling points per iteration $\mathcal{N}$ of 10^8, 10^9, and even 10^{10}. The results show no sign of the central values drifting beyond the error bars estimated by VEGAS as $\mathcal{N}$ increases. We are therefore confident that our result (31) is free from the problem caused by insufficient samplings.

TABLE V. Contributions of diagrams of Set I(i) to a_μ for $(l_1 l_2) = (mt)$. The multiplicity n_F is the number of vertex diagrams represented by the integral and is incorporated in the numerical value. The superscript (mt) is omitted for simplicity.

Integral	n_F	Value (Error) including n_F	Sampling per iteration	Number of iterations
$M_{2,p01}$	1	0.000 173 73 (5)	1×10^8	50
$M_{2,p02}$	1	0.000 115 02 (4)	1×10^8	50
$M_{2,p03}$	1	0.000 299 06 (8)	1×10^8	50
$M_{2,p04}$	2	0.000 220 89 (9)	1×10^8	50
$M_{2,p05}$	2	0.000 354 37 (21)	1×10^8	50
$M_{2,p06}$	2	0.000 725 06 (24)	1×10^8	50
$M_{2,p07}$	2	0.000 730 62 (28)	1×10^8	50
$M_{2,p08}$	2	0.000 599 02 (19)	1×10^8	50
$M_{2,p09}$	2	−0.000 221 58 (10)	1×10^8	50
$M_{2,p10}$	2	−0.000 370 54 (12)	1×10^8	50
$M_{2,p11}$	2	0.000 107 04 (3)	1×10^8	50
$M_{2,p12}$	2	0.000 252 11 (6)	1×10^8	50
$M_{2,p13}$	2	0.000 079 35 (18)	1×10^8	50
$M_{2,p14}$	2	0.000 610 34 (18)	1×10^8	50
$M_{2,p15}$	2	0.000 064 07 (1)	1×10^8	50
$M_{2,p16}$	2	0.000 097 35 (2)	1×10^8	50
$M_{2,p17}$	2	−0.000 066 71 (3)	1×10^8	50
$M_{2,p18}$	2	0.000 056 95 (3)	1×10^8	50
$M_{2,p19}$	2	0.000 132 63 (4)	1×10^8	50
$M_{2,p20}$	2	0.000 170 72 (2)	1×10^8	50
$M_{2,p21}$	2	−0.000 093 37 (3)	1×10^8	50
$M_{2,p22}$	2	0.000 071 59 (4)	1×10^8	50
$M_{2,p23}$	4	0.000 051 80 (4)	1×10^8	50
$M_{2,p24}$	4	0.000 222 52 (11)	1×10^8	50
$M_{2,p25}$	4	0.000 975 69 (35)	1×10^8	50
$M_{2,p26}$	4	−0.000 352 91 (15)	1×10^8	50
$M_{2,p27}$	4	−0.000 737 37 (32)	1×10^8	50
$M_{2,p28}$	4	−0.000 517 81 (17)	1×10^8	50
$M_{2,p29}$	4	0.000 584 31 (32)	1×10^8	50
$M_{2,p30}$	4	0.001 408 74 (49)	1×10^8	50
$M_{2,p31}$	4	−0.000 768 96 (38)	1×10^8	50
$M_{2,p32}$	4	−0.000 714 49 (14)	1×10^8	50
$M_{2,p33}$	4	0.000 220 34 (10)	1×10^8	50
$M_{2,p34}$	4	−0.000 000 59 (8)	1×10^8	50
$M_{2,p35}$	4	−0.000 257 99 (13)	1×10^8	50
$M_{2,p36}$	4	−0.000 820 21 (17)	1×10^8	50
$M_{2,p37}$	4	−0.000 741 52 (19)	1×10^8	50
$M_{2,p38}$	4	−0.000 269 58 (22)	1×10^8	50
$M_{2,p39}$	4	−0.000 065 68 (4)	1×10^8	50

ACKNOWLEDGMENTS

This work is supported in part by the JSPS Grant-in-Aid for Scientific Research (C)19540322 and (C)20540261. T. K.'s work is supported in part by the U. S. National Science Foundation under Grant No. NSF-PHY-0757868, and the International Exchange Support Grants (FY2010) of RIKEN. T. K. thanks RIKEN for the hospitality extended to him while a part of this work was carried out. Numerical calculations are conducted in part on the RIKEN Super Combined Cluster System (RSCC) and the RIKEN Integrated Cluster of Clusters (RICC) supercomputing systems.

Note added in proof.—In order to test the assumption that the difference of (31) and (36) is caused by the $O(m_e/m_\mu)$ term of (36) we carried out an additional computation of the electron-loop contribution to the tau lepton $g-2$, and obtained

$$a_\tau^{(10)}[\mathrm{I(i)}^{(te)}\text{:num.}] = -0.212\,(41).$$

Meanwhile the asymptotic calculation gives

$$a_\tau^{(10)}[\mathrm{I(i)}^{(te)}\text{:asym.}] = -0.255 + O(m_e/m_\tau).$$

This implies that the term of order m_e/m_τ is about +0.043 (41). Although this is not as small as is implied by the ratio m_μ/m_τ times 0.17 of Eq. (41), it is consistent with the expected behavior within the error bars.

APPENDIX A: FOURTH-ORDER VACUUM-POLARIZATION FUNCTIONS WITH MASS INSERTION AND THEIR CONTRIBUTION TO $M_{2,P_{4^*}}$

Since $M_{2,\Delta P_{4^*}}$ does not appear except in Set I(i) in our study of the tenth-order $g-2$, we shall derive parametric formulas for the diagrams Π_{4a^*}, Π_{4b^*}, and $M_{2,P_{4^*}}$ in this appendix.

Our derivation follows closely the treatment of diagrams $\Pi_{4a}^{\mu\nu}$ and $\Pi_{4b}^{\mu\nu}$ (without mass insertion) which consist of four lepton lines forming a closed loop and an internal photon line a as shown in Fig. 5. Following the steps leading to Eq. (14) we obtain

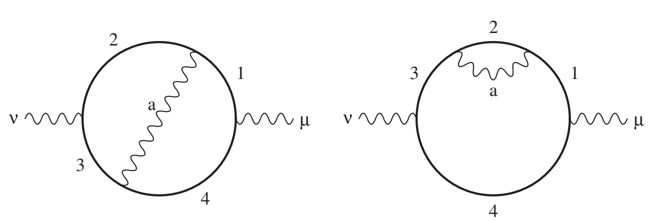

(a)Π_{4a} (b)Π_{4b}

FIG. 5. Fourth-order vacuum-polarization diagrams.

$$\Pi_{4^*}^{\mu\nu} = +2\left(\frac{-1}{4}\right)^2 \int \frac{(dz)}{U^2}\left(\sum_j \pm z_j D_j^\mu\right) \times \mathrm{Tr}[\not q(\not D_i + m)\cdots\gamma^\nu\cdots]\frac{1}{V^3}. \tag{A1}$$

From Lorentz invariance and gauge invariance, we have the general structure

$$\Pi_{4^*}^{\mu\nu} = (q_\mu q_\nu - q^2 g_{\mu\nu})\tilde{\Pi}_{4^*} + (\text{gauge-dependent terms}). \tag{A2}$$

Charge renormalization is achieved by

$$\Pi_{4^*}(q^2) = \tilde{\Pi}_{4^*}(q^2) - \tilde{\Pi}_{4^*}(0). \tag{A3}$$

When the D operation is carried out in $\tilde{\Pi}_{4^*}$, the result can be expressed in the form

$$\Pi_{4^*}(q^2) = \int(dz)\left[\frac{D_0}{U^2}\left(\frac{1}{V^2} - \frac{1}{V_0^2}\right) + \frac{q^2 B_0}{V^2} + \frac{D_1}{U^3}\left(\frac{1}{V} - \frac{1}{V_0}\right)\right], \tag{A4}$$

where $V_0 = z_{1234}m^2$ and D_0, B_0, D_1, U, V, and (dz) are diagram-specific.

1. Diagram $M_{2,P_{4a^*}}$

This diagram has four fermion lines into which mass vertex can be inserted. They all give the same contribution to $M_{2,P_{4a^*}}$ so that we have to evaluate only one of them such as $\Pi_{4a,1^*}$ of Fig. 6(a). For this diagram we find

$$\begin{aligned} D_0 &= r^4(-2A_3A_4 - 2A_2A_4 + A_2A_3 + 2A_1A_4 - A_1A_3 - A_1A_2),\\ B_0 &= r^2A_4^2(A_2A_3 - A_1A_3 - A_1A_2),\\ D_1 &= r^2B_{11}(A_3A_4 + A_2A_4 + 2A_1A_3 + 2A_1A_2)\\ &\quad + r^2B_{12}(-3A_3A_4 - A_2A_4 + 2A_1A_4 - 2A_1A_2)\\ &\quad + r^2B_{22}(2A_1A_4), \end{aligned} \tag{A5}$$

where r is the ratio of the mass m of the loop lepton and the mass of the lepton of M_2 and

$$\begin{aligned} &A_1 = 1 - z_1B_{11} - z_2B_{12}, \quad A_2 = 1 - z_1B_{12} - z_2B_{22},\\ &A_3 = -z_1B_{13} - z_2B_{23}, \quad A_4 = -z_1B_{14} - z_2B_{24},\\ &B_{11} = z_{23a}, \quad B_{12} = z_a, \quad B_{22} = z_{14a},\\ &U = z_{14a}z_{23} + z_{14}z_a, \quad G = z_1A_1 + z_2A_2,\\ &V = V_0 - q^2G,\\ &(dz) = z_1dz_1dz_2dz_3dz_4dz_a\delta(1 - z_{1234a}), \quad z_i \geq 0. \end{aligned} \tag{A6}$$

This diagram has a UV divergence from the subvertex $\{2, 3, a\}$, which can be isolated by the K_{23} operation. Subtraction of this term yields a UV-finite value

$$\Delta\Pi_{4a^*} = 4(1 - K_{23})\Pi_{4a,1^*}, \tag{A7}$$

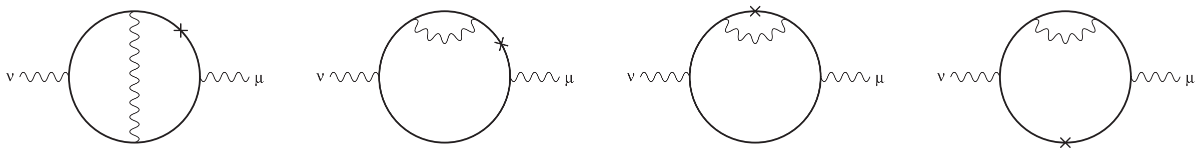

(a)$\Pi_{4a,1^*}$ (b)$\Pi_{4b,1^*}$ (c)$\Pi_{4b,2^*}$ (d)$\Pi_{4b,4^*}$

FIG. 6. Fourth-order vacuum-polarization diagrams with mass insertions.

and a finite contribution $M_{2,P_{4a^*}}$ to $g-2$. By numerical integration we obtain the value $-0.066\,907\,(7)$ for the (ee) case, and $-0.443\,935\,(69)$ for the (me) case.

2. Diagram $M_{2,P_{4b^*}}$

The diagrams $\Pi_{4b,1^*}$ and $\Pi_{4b,3^*}$ give an identical contribution to $M_{2,P_{4b^*}}$, whereas the diagrams $\Pi_{4b,2^*}$ and $\Pi_{4b,4^*}$ must be treated separately.

For the diagrams $\Pi_{4b,1^*}$ [see Fig. 6(b)] we find

$$\begin{aligned} D_0 &= r^4(2A_2A_4-6A_1A_4),\\ B_0 &= r^2(3A_1^2A_2A_4-2A_1^3A_4),\\ D_1 &= r^2B_{11}(6A_1A_4-A_1A_2+2A_1^2)+r^2B_{12}(-9A_1A_4-2A_1^2), \end{aligned} \tag{A8}$$

where

$$\begin{aligned} &A_1 = 1-z_1B_{11}-z_2B_{12}-z_3B_{13},\\ &A_2 = 1-z_1B_{12}-z_2B_{22}-z_3B_{23},\\ &A_3 = A_1, \qquad A_4 = A_1-1,\\ &B_{11} = B_{13} = B_{14} = B_{33} = B_{34} = B_{44} = z_{2a},\\ &B_{12} = B_{23} = B_{24} = z_a, \qquad B_{22} = z_{134a},\\ &U = z_{134}z_{2a}+z_2z_a, \qquad G = z_1A_1+z_2A_2+z_3A_3,\\ &V = V_0-q^2G,\\ &(dz) = z_1dz_1dz_2dz_3dz_4dz_a\delta(1-z_{1234a}), \qquad z_i\geq 0. \end{aligned} \tag{A9}$$

This diagram has a UV divergence from the self-energy subdiagram $\{2,a\}$ which can be subtracted by the K_2 operation

$$\Delta\Pi_{4b,1^*} = (1-K_2)\Pi_{4b,1^*}. \tag{A10}$$

For the diagrams $\Pi_{4b,2^*}$ [see Fig. 6(c)] we find

$$\begin{aligned} D_0 &= r^4(2A_2A_4-4A_1A_4),\\ B_0 &= r^2(-4A_1A_2^2A_4+2A_1^2A_2A_4),\\ D_1 &= r^2B_{22}(8A_1A_4)+r^2B_{11}(2A_2A_4)\\ &\quad + r^2B_{12}(4A_2A_4-8A_1A_4+4A_1A_2-2A_1^2), \end{aligned} \tag{A11}$$

where

$$\begin{aligned} &A_1 = 1-z_1B_{11}-z_2B_{12}-z_3B_{13},\\ &A_2 = 1-z_1B_{12}-z_2B_{22}-z_3B_{23},\\ &A_3 = 1-z_1B_{13}-z_2B_{23}-z_3B_{33},\\ &A_4 = -z_1B_{14}-z_2B_{24}-z_3B_{34},\\ &B_{11} = B_{13} = B_{14} = B_{33} = B_{34} = B_{44} = z_{2a},\\ &B_{12} = B_{23} = B_{24} = z_a, \qquad B_{22} = z_{134a},\\ &U = z_{134}z_{2a}+z_2z_a, \qquad G = z_1A_1+z_2A_2+z_3A_3,\\ &V = V_0-q^2G,\\ &(dz) = z_2dz_1dz_2dz_3dz_4dz_a\delta(1-z_{1234a}), \qquad z_i\geq 0. \end{aligned} \tag{A12}$$

This diagram has a UV divergence from the subdiagram $\{2^*,a\}$ which can be subtracted by the K_{2^*} operation

$$\Delta\Pi_{4b,2^*} = (1-K_{2^*})\Pi_{4b,2^*}. \tag{A13}$$

For the diagrams $\Pi_{4b,4^*}$ [see Fig. 6(d)] we find

$$\begin{aligned} D_0 &= r^4(2A_2A_4-8A_1A_4), \qquad B_0 = r^2(2A_1^2A_2A_4),\\ D_1 &= r^2B_{11}(2A_2A_4)+r^2B_{12}(-8A_1A_4-2A_1^2), \end{aligned} \tag{A14}$$

where

$$\begin{aligned} &A_1 = 1-z_1B_{11}-z_2B_{12}-z_3B_{13},\\ &A_2 = 1-z_1B_{12}-z_2B_{22}-z_3B_{23},\\ &A_3 = 1-z_1B_{13}-z_2B_{23}-z_3B_{33},\\ &A_4 = -z_1B_{14}-z_2B_{24}-z_3B_{34},\\ &B_{11} = B_{13} = B_{14} = B_{33} = B_{34} = B_{44} = z_{2a},\\ &B_{12} = B_{23} = B_{24} = z_a, \qquad B_{22} = z_{134a},\\ &U = z_{134}z_{2a}+z_2z_a, \qquad G = z_1A_1+z_2A_2+z_3A_3,\\ &V = V_0-q^2G,\\ &(dz) = z_4dz_1dz_2dz_3dz_4dz_a\delta(1-z_{1234a}), \qquad z_i\geq 0. \end{aligned} \tag{A15}$$

As is for the diagram $\Pi_{4b,1^*}$ this diagram has a UV divergence from the self-energy subdiagram $\{2,a\}$ which can be subtracted by the K_2 operation.

By numerical integration we obtain for the (ee) case

$$2M^{(ee)}_{2,\Delta P_{4b^*}} = -0.046\,309\,(7) + 0.033\,507\,(4) - 0.038\,061\,(6) = -0.050\,863\,(9), \tag{A16}$$

where the right-hand side of the first line is listed in order of $P_{4b,1^*}$, $P_{4b,2^*}$, and $P_{4b,4^*}$.

The result for the (me) case is

$$2M^{(me)}_{2,\Delta P_{4b^*}} = -0.409\,550\,(61) + 0.528\,759\,(51) - 0.429\,683\,(62) = -0.310\,464\,(101). \tag{A17}$$

The sums $M_{2,\Delta P_{4^*}} \equiv M_{2,\Delta P_{4a^*}} + 2M_{2,\Delta P_{4b^*}}$ for the (ee), (em), (me), and (mt) cases are listed in Table II.

APPENDIX B: STANDARD ON-THE-MASS-SHELL RENORMALIZATION

This appendix describes the standard on-the-mass-shell renormalization of vacuum-polarization function $\Pi^{(n)}$, where $n = 2, 4, 6, 8$. $\Pi^{(2)}$ consists of only one diagram, but higher order functions consist of several diagrams, which must be distinguished by an additional symbol. For instance $\Pi^{(4i)}$ with $i = a, b$, $\Pi^{(6j)}$ with $j = A, B, \ldots, H$. However, the eighth-order functions are denoted as $\Pi^{(k)}$, $k = p01, p02, \ldots, p39$ to avoid overcrowding.

Renormalization terms include functions such as $\Pi^{(2^*)}$ which means insertion of a two-point vertex (such as a mass vertex) in the fermion line.

Quantities L_n, B_n, δm_n denote a vertex renormalization constant, wave-function renormalization constant, mass renormalization constant of nth order of the standard on-the-mass-shell renormalization, respectively. We must also deal with renormalization constants with mass insertion. For instance for L_2, which contains two electron lines, it is necessary to distinguish the lines into which a two-point vertex insertion is made. Suppose we name them line 1 and line 2. Then $L_{2(1^*1^*)}$ implies that two two-point vertices are inserted in the fermion line 1 of L_2, while $L_{2(1^*2^*)}$ means that one two-point vertex is inserted in line 1 while another is inserted in line 2. (Previously [25] we used the notations $L_{2^{**\dagger}}$ and $L_{2^{*\dagger *}}$ for these quantities.)

1. Standard renormalization of fourth-order vacuum polarization

$$\Pi^{(4a)}_{\rm ren} = \Pi^{(4a)} - 2L_2\Pi^{(2)},$$

$$\Pi^{(4b)}_{\rm ren} = \Pi^{(4b)} - \delta m_2\Pi^{(2*)} - B_2\Pi^{(2)}.$$

2. Standard renormalization of sixth-order vacuum polarization

$$\Pi^{(6A)}_{\rm ren} = \Pi^{(6A)} + 2\delta m_2B_2\Pi^{(2*)} - 2\delta m_2\Pi^{(4b,1*)} + (\delta m_2)^2\Pi^{(2**)} - 2B_2\Pi^{(4b)} + (B_2)^2\Pi^{(2)},$$

$$\Pi^{(6B)}_{\rm ren} = \Pi^{(6B)} + 2\delta m_2B_2\Pi^{(2*)} - 2\delta m_2\Pi^{(4b,4*)} + (\delta m_2)^2\Pi^{(2**)} - 2B_2\Pi^{(4b)} + (B_2)^2\Pi^{(2)},$$

$$\Pi^{(6C)}_{\rm ren} = \Pi^{(6C)} - \delta m_{4b}\Pi^{(2*)} + \delta m_{2*}\delta m_2\Pi^{(2*)} + \delta m_2B_{2*}\Pi^{(2)} + \delta m_2B_2\Pi^{(2*)} - \delta m_2\Pi^{(4b,2*)} - B_{4b}\Pi^{(2)} - B_2\Pi^{(4b)} + (B_2)^2\Pi^{(2)},$$

$$\Pi^{(6D)}_{\rm ren} = \Pi^{(6D)} - \delta m_{4a}\Pi^{(2*)} + 2\delta m_2L_2\Pi^{(2*)} - B_{4a}\Pi^{(2)} + 2B_2L_2\Pi^{(2)} - 2L_2\Pi^{(4b)},$$

$$\Pi^{(6E)}_{\rm ren} = \Pi^{(6E)} + \delta m_2L_{2*}\Pi^{(2)} + \delta m_2L_2\Pi^{(2*)} - \delta m_2\Pi^{(4a,1*)} + 2B_2L_2\Pi^{(2)} - B_2\Pi^{(4a)} - L_{4b,1}\Pi^{(2)} - L_2\Pi^{(4b)},$$

$$\Pi^{(6F)}_{\rm ren} = \Pi^{(6F)} - 2L_{4a,1}\Pi^{(2)} - L_2\Pi^{(4a)} + 2(L_2)^2\Pi^{(2)},$$

$$\Pi^{(6G)}_{\rm ren} = \Pi^{(6G)} - 2L_{4b,2}\Pi^{(2)} - 2L_2\Pi^{(4a)} + 3(L_2)^2\Pi^{(2)},$$

$$\Pi^{(6H)}_{\rm ren} = \Pi^{(6H)} - 2L_{4a,2}\Pi^{(2)}.$$

3. Standard renormalization of eighth-order vacuum polarization

$$\Pi^{(p01)}_{\rm ren} = \Pi^{(p01)} - 2L_{6F,3}\Pi^{(2)} + 4L_{4a,1}L_2\Pi^{(2)} - 2L_2\Pi^{(6F)} + (L_2)^2\Pi^{(4a)} - 2(L_2)^3\Pi^{(2)},$$

$$\Pi^{(p02)}_{\rm ren} = \Pi^{(p02)} - 2L_{6H,3}\Pi^{(2)},$$

$$\Pi^{(p03)}_{\rm ren} = \Pi^{(p03)} - 2L_{6B,3}\Pi^{(2)} + 6L_{4b,2}L_2\Pi^{(2)} - 2L_{4b,2}\Pi^{(4a)} - 2L_2\Pi^{(6G)} + 3(L_2)^2\Pi^{(4a)} - 4(L_2)^3\Pi^{(2)},$$

$$\Pi^{(p04)}_{\rm ren} = \Pi^{(p04)} + 6\delta m_2B_2\Pi^{(4b,1*)} - 3\delta m_2(B_2)^2\Pi^{(2*)} - \delta m_2\Pi^{(6A,3*)} - 2\delta m_2\Pi^{(6A,1*)} - 3(\delta m_2)^2B_2\Pi^{(2**)} + (\delta m_2)^2\Pi^{(4b,1*3*)} + 2(\delta m_2)^2\Pi^{(4b,1*1*)} - (\delta m_2)^3\Pi^{(2***)} - 3B_2\Pi^{(6A)} + 3(B_2)^2\Pi^{(4b)} - (B_2)^3\Pi^{(2)},$$

$$\Pi^{(p05)}_{\rm ren} = \Pi^{(p05)} + 4\delta m_2 B_2 \Pi^{(4b,4*)} + 2\delta m_2 B_2 \Pi^{(4b,1*)} - 3\delta m_2 (B_2)^2 \Pi^{(2*)} - 2\delta m_2 \Pi^{(6B,1*)} - \delta m_2 \Pi^{(6A,6*)} - 2(\delta m_2)^2 B_2 \Pi^{(2**)} - (\delta m_2)^2 B_2 \Pi^{(2**)} + (\delta m_2)^2 \Pi^{(4b,4*4*)} + 2(\delta m_2)^2 \Pi^{(4b,1*4*)} - (\delta m_2)^3 \Pi^{(2***)} - 2B_2 \Pi^{(6B)} - B_2 \Pi^{(6A)} + 3(B_2)^2 \Pi^{(4b)} - (B_2)^3 \Pi^{(2)},$$

$$\Pi^{(p06)}_{\rm ren} = \Pi^{(p06)} - 2\delta m_2 B_2 L_{2*} \Pi^{(2)} - 2\delta m_2 B_2 L_2 \Pi^{(2*)} + 2\delta m_2 B_2 \Pi^{(4a,1*)} + 2\delta m_2 L_{4b,1} \Pi^{(2*)} + 2\delta m_2 L_{2*} \Pi^{(4b)} - 2\delta m_2 \Pi^{(6E,1*)} - 2(\delta m_2)^2 L_{2*} \Pi^{(2*)} + (\delta m_2)^2 \Pi^{(4a,1*2*)} + 2B_2 L_{4b,1} \Pi^{(2)} + 2B_2 L_2 \Pi^{(4b)} - 2B_2 \Pi^{(6E)} - 2(B_2)^2 L_2 \Pi^{(2)} + (B_2)^2 \Pi^{(4a)} - 2L_{4b,1} \Pi^{(4b)},$$

$$\Pi^{(p07)}_{\rm ren} = \Pi^{(p07)} - 2\delta m_2 B_2 L_{2*} \Pi^{(2)} - 2\delta m_2 B_2 L_2 \Pi^{(2*)} + 2\delta m_2 B_2 \Pi^{(4a,1*)} + 2\delta m_2 L_{4b,1(1*)} \Pi^{(2)} + 2\delta m_2 L_2 \Pi^{(4b,4*)} - 2\delta m_2 \Pi^{(6E,5*)} - (\delta m_2)^2 L_{2(1*2*)} \Pi^{(2)} - (\delta m_2)^2 L_2 \Pi^{(2**)} + (\delta m_2)^2 \Pi^{(4a,1*4*)} + 2B_2 L_{4b,1} \Pi^{(2)} + 2B_2 L_2 \Pi^{(4b)} - 2B_2 \Pi^{(6E)} - 2(B_2)^2 L_2 \Pi^{(2)} + (B_2)^2 \Pi^{(4a)} - L_{6A,3} \Pi^{(2)} - L_2 \Pi^{(6B)},$$

$$\Pi^{(p08)}_{\rm ren} = \Pi^{(p08)} - 2\delta m_2 B_2 L_{2*} \Pi^{(2)} - 2\delta m_2 B_2 L_2 \Pi^{(2*)} + 2\delta m_2 B_2 \Pi^{(4a,1*)} + 2\delta m_2 L_{4b,1} \Pi^{(2*)} + 2\delta m_2 L_{2*} \Pi^{(4b)} - 2\delta m_2 \Pi^{(6E,6*)} - 2(\delta m_2)^2 L_{2*} \Pi^{(2*)} + (\delta m_2)^2 \Pi^{(4a,1*3*)} + 2B_2 L_{4b,1} \Pi^{(2)} + 2B_2 L_2 \Pi^{(4b)} - 2B_2 \Pi^{(6E)} - 2(B_2)^2 L_2 \Pi^{(2)} + (B_2)^2 \Pi^{(4a)} - 2L_{4b,1} \Pi^{(4b)},$$

$$\Pi^{(p09)}_{\rm ren} = \Pi^{(p09)} + \delta m_{4a} \delta m_2 \Pi^{(2**)} + \delta m_{4a} B_2 \Pi^{(2*)} - \delta m_{4a} \Pi^{(4b,4*)} + \delta m_2 B_{4a} \Pi^{(2*)} - 4\delta m_2 B_2 L_2 \Pi^{(2*)} + 4\delta m_2 L_2 \Pi^{(4b,4*)} - \delta m_2 \Pi^{(6D,6*)} - 2(\delta m_2)^2 L_2 \Pi^{(2**)} + B_{4a} B_2 \Pi^{(2)} - B_{4a} \Pi^{(4b)} + 4B_2 L_2 \Pi^{(4b)} - B_2 \Pi^{(6D)} - 2(B_2)^2 L_2 \Pi^{(2)} - 2L_2 \Pi^{(6B)},$$

$$\Pi^{(p10)}_{\rm ren} = \Pi^{(p10)} + \delta m_{4b} \delta m_2 \Pi^{(2**)} + \delta m_{4b} B_2 \Pi^{(2*)} - \delta m_{4b} \Pi^{(4b,4*)} - \delta m_{2*} \delta m_2 B_2 \Pi^{(2*)} + \delta m_{2*} \delta m_2 \Pi^{(4b,4*)} - \delta m_{2*} (\delta m_2)^2 \Pi^{(2**)} + \delta m_2 B_{4b} \Pi^{(2*)} - \delta m_2 B_{2*} B_2 \Pi^{(2)} + \delta m_2 B_{2*} \Pi^{(4b)} + 2\delta m_2 B_2 \Pi^{(4b,4*)} + \delta m_2 B_2 \Pi^{(4b,2*)} - 2\delta m_2 (B_2)^2 \Pi^{(2*)} - \delta m_2 \Pi^{(6C,6*)} - \delta m_2 \Pi^{(6B,2*)} - (\delta m_2)^2 B_{2*} \Pi^{(2*)} - (\delta m_2)^2 B_2 \Pi^{(2**)} + (\delta m_2)^2 \Pi^{(4b,2*4*)} + B_{4b} B_2 \Pi^{(2)} - B_{4b} \Pi^{(4b)} - B_2 \Pi^{(6C)} - B_2 \Pi^{(6B)} + 2(B_2)^2 \Pi^{(4b)} - (B_2)^3 \Pi^{(2)},$$

$$\Pi^{(p11)}_{\rm ren} = \Pi^{(p11)} - \delta m_{6F} \Pi^{(2*)} + 2\delta m_{4a} L_2 \Pi^{(2*)} + 2\delta m_2 L_{4a,1} \Pi^{(2*)} - 3\delta m_2 (L_2)^2 \Pi^{(2*)} - B_{6F} \Pi^{(2)} + 2B_{4a} L_2 \Pi^{(2)} + 2B_2 L_{4a,1} \Pi^{(2)} - 3B_2 (L_2)^2 \Pi^{(2)} - 2L_{4a,1} \Pi^{(4b)} - 2L_2 \Pi^{(6D)} + 3(L_2)^2 \Pi^{(4b)},$$

$$\Pi^{(p12)}_{\rm ren} = \Pi^{(p12)} - \delta m_{6A} \Pi^{(2*)} + 2\delta m_{4b(1*)} \delta m_2 \Pi^{(2*)} + 2\delta m_{4b} B_2 \Pi^{(2*)} - \delta m_{2**} (\delta m_2)^2 \Pi^{(2*)} - 2\delta m_{2*} \delta m_2 B_2 \Pi^{(2*)} + 2\delta m_2 B_{4b(1*)} \Pi^{(2)} - 2\delta m_2 B_{2*} B_2 \Pi^{(2)} + 2\delta m_2 B_2 \Pi^{(4b,2*)} - \delta m_2 (B_2)^2 \Pi^{(2*)} - 2\delta m_2 \Pi^{(6C,2*)} - (\delta m_2)^2 B_{2**} \Pi^{(2)} + (\delta m_2)^2 \Pi^{(4b,2*2*)} - B_{6A} \Pi^{(2)} + 2B_{4b} B_2 \Pi^{(2)} - 2B_2 \Pi^{(6C)} + (B_2)^2 \Pi^{(4b)} - (B_2)^3 \Pi^{(2)},$$

$$\Pi^{(p13)}_{\rm ren} = \Pi^{(p13)} + 2\delta m_2 L_{4a,2(1*)} \Pi^{(2)} - \delta m_2 \Pi^{(6H,2*)} + 2B_2 L_{4a,2} \Pi^{(2)} - B_2 \Pi^{(6H)} - 2L_{6D,4} \Pi^{(2)},$$

$$\Pi^{(p14)}_{\rm ren} = \Pi^{(p14)} + 2\delta m_2 L_{4b,2(1*)} \Pi^{(2)} - 2\delta m_2 L_{2*} L_2 \Pi^{(2)} + 2\delta m_2 L_2 \Pi^{(4a,1*)} - \delta m_2 (L_2)^2 \Pi^{(2*)} - \delta m_2 \Pi^{(6G,2*)} + 2B_2 L_{4b,2} \Pi^{(2)} + 2B_2 L_2 \Pi^{(4a)} - 3B_2 (L_2)^2 \Pi^{(2)} - B_2 \Pi^{(6G)} - 2L_{6A,2} \Pi^{(2)} + 2L_{4b,1} L_2 \Pi^{(2)} - 2L_2 \Pi^{(6E)} + (L_2)^2 \Pi^{(4b)},$$

$$\Pi^{(p15)}_{\rm ren} = \Pi^{(p15)} - \delta m_{6H} \Pi^{(2*)} + 2\delta m_2 L_{4a,2} \Pi^{(2*)} - B_{6H} \Pi^{(2)} + 2B_2 L_{4a,2} \Pi^{(2)} - 2L_{4a,2} \Pi^{(4b)},$$

$$\Pi^{(p16)}_{\rm ren} = \Pi^{(p16)} - 2L_{6H,1} \Pi^{(2)} + 2L_{4a,2} L_2 \Pi^{(2)} - L_{4a,2} \Pi^{(4a)},$$

$$\Pi_{\rm ren}^{(p17)} = \Pi^{(p17)} - 2L_{6H,2}\Pi^{(2)},$$

$$\Pi_{\rm ren}^{(p18)} = \Pi^{(p18)} - 2L_{6G,2}\Pi^{(2)},$$

$$\Pi_{\rm ren}^{(p19)} = \Pi^{(p19)} - 2L_{6G,5}\Pi^{(2)} + 2L_{4b,2}L_2\Pi^{(2)} - L_{4b,2}\Pi^{(4a)} + 2L_{4a,1}L_2\Pi^{(2)} - L_2\Pi^{(6F)} + (L_2)^2\Pi^{(4a)} - 2(L_2)^3\Pi^{(2)},$$

$$\begin{aligned}\Pi_{\rm ren}^{(p20)} = {} & \Pi^{(p20)} - \delta m_{6C}\Pi^{(2*)} + 2\delta m_{4b}L_2\Pi^{(2*)} + \delta m_{4a}\delta m_{2*}\Pi^{(2*)} + \delta m_{4a}B_{2*}\Pi^{(2)} - \delta m_{4a}\Pi^{(4b,2*)} \\ & - 2\delta m_{2*}\delta m_2 L_2\Pi^{(2*)} + \delta m_2 B_{4a}\Pi^{(2*)} - 2\delta m_2 B_{2*}L_2\Pi^{(2)} - 2\delta m_2 B_2 L_2\Pi^{(2*)} + 2\delta m_2 L_2\Pi^{(4b,2*)} - B_{6C}\Pi^{(2)} \\ & + 2B_{4b}L_2\Pi^{(2)} + B_{4a}B_2\Pi^{(2)} - B_{4a}\Pi^{(4b)} + 2B_2L_2\Pi^{(4b)} - 2(B_2)^2L_2\Pi^{(2)} - 2L_2\Pi^{(6C)},\end{aligned}$$

$$\begin{aligned}\Pi_{\rm ren}^{(p21)} = {} & \Pi^{(p21)} - \delta m_{6E}\Pi^{(2*)} + \delta m_{4a(2*)}\delta m_2\Pi^{(2*)} + \delta m_{4a}B_2\Pi^{(2*)} + \delta m_2 B_{4a(2*)}\Pi^{(2)} - 2\delta m_2 B_2 L_{2*}\Pi^{(2)} \\ & - 2\delta m_2 B_2 L_2\Pi^{(2*)} + 2\delta m_2 L_{4b,1}\Pi^{(2*)} + 2\delta m_2 L_{2*}\Pi^{(4b)} - \delta m_2\Pi^{(6D,3*)} - 2(\delta m_2)^2 L_{2*}\Pi^{(2*)} - B_{6E}\Pi^{(2)} \\ & + B_{4a}B_2\Pi^{(2)} + 2B_2L_{4b,1}\Pi^{(2)} + 2B_2L_2\Pi^{(4b)} - B_2\Pi^{(6D)} - 2(B_2)^2L_2\Pi^{(2)} - 2L_{4b,1}\Pi^{(4b)},\end{aligned}$$

$$\begin{aligned}\Pi_{\rm ren}^{(p22)} = {} & \Pi^{(p22)} - \delta m_{6B}\Pi^{(2*)} + \delta m_{4b(2*)}\delta m_2\Pi^{(2*)} + \delta m_{4b}\delta m_{2*}\Pi^{(2*)} + \delta m_{4b}B_{2*}\Pi^{(2)} + \delta m_{4b}B_2\Pi^{(2*)} - \delta m_{4b}\Pi^{(4b,2*)} \\ & - \delta m_{2*}\delta m_2 B_{2*}\Pi^{(2)} - \delta m_{2*}\delta m_2 B_2\Pi^{(2*)} + \delta m_{2*}\delta m_2\Pi^{(4b,2*)} - (\delta m_{2*})^2\delta m_2\Pi^{(2*)} + \delta m_2 B_{4b(2*)}\Pi^{(2)} \\ & + \delta m_2 B_{4b}\Pi^{(2*)} - 2\delta m_2 B_{2*}B_2\Pi^{(2)} + \delta m_2 B_{2*}\Pi^{(4b)} + \delta m_2 B_2\Pi^{(4b,2*)} - \delta m_2(B_2)^2\Pi^{(2*)} - \delta m_2\Pi^{(6C,3*)} \\ & - (\delta m_2)^2 B_{2*}\Pi^{(2*)} - B_{6B}\Pi^{(2)} + 2B_{4b}B_2\Pi^{(2)} - B_{4b}\Pi^{(4b)} - B_2\Pi^{(6C)} + (B_2)^2\Pi^{(4b)} - (B_2)^3\Pi^{(2)},\end{aligned}$$

$$\Pi_{\rm ren}^{(p23)} = \Pi^{(p23)} - 2L_{6G,3}\Pi^{(2)},$$

$$\Pi_{\rm ren}^{(p24)} = \Pi^{(p24)} - L_{6E,3}\Pi^{(2)} - L_{6C,3}\Pi^{(2)} + 3L_{4a,2}L_2\Pi^{(2)} - L_{4a,2}\Pi^{(4a)} - L_2\Pi^{(6H)},$$

$$\begin{aligned}\Pi_{\rm ren}^{(p25)} = {} & \Pi^{(p25)} - 2\delta m_2 B_2 L_{2*}\Pi^{(2)} - 2\delta m_2 B_2 L_2\Pi^{(2*)} + 2\delta m_2 B_2\Pi^{(4a,1*)} + \delta m_2 L_{4b,1(4*)}\Pi^{(2)} + \delta m_2 L_{4b,1(2*)}\Pi^{(2)} \\ & + 2\delta m_2 L_2\Pi^{(4b,1*)} - \delta m_2\Pi^{(6E,4*)} - \delta m_2\Pi^{(6E,2*)} - (\delta m_2)^2 L_{2(1*1*)}\Pi^{(2)} - (\delta m_2)^2 L_2\Pi^{(2**)} + (\delta m_2)^2\Pi^{(4a,1*1*)} \\ & + 2B_2L_{4b,1}\Pi^{(2)} + 2B_2L_2\Pi^{(4b)} - 2B_2\Pi^{(6E)} - 2(B_2)^2L_2\Pi^{(2)} + (B_2)^2\Pi^{(4a)} - L_{6A,1}\Pi^{(2)} - L_2\Pi^{(6A)},\end{aligned}$$

$$\begin{aligned}\Pi_{\rm ren}^{(p26)} = {} & \Pi^{(p26)} + \delta m_{4a}\delta m_2\Pi^{(2**)} + \delta m_{4a}B_2\Pi^{(2*)} - \delta m_{4a}\Pi^{(4b,1*)} + \delta m_2 B_{4a}\Pi^{(2*)} - 4\delta m_2 B_2 L_2\Pi^{(2*)} \\ & + 4\delta m_2 L_2\Pi^{(4b,1*)} - \delta m_2\Pi^{(6D,1*)} - 2(\delta m_2)^2 L_2\Pi^{(2**)} + B_{4a}B_2\Pi^{(2)} - B_{4a}\Pi^{(4b)} + 4B_2L_2\Pi^{(4b)} - B_2\Pi^{(6D)} \\ & - 2(B_2)^2L_2\Pi^{(2)} - 2L_2\Pi^{(6A)},\end{aligned}$$

$$\begin{aligned}\Pi_{\rm ren}^{(p27)} = {} & \Pi^{(p27)} + \delta m_2 L_{4a,1(2*)}\Pi^{(2)} + \delta m_2 L_{4a,1}\Pi^{(2*)} - \delta m_2 L_{2*}L_2\Pi^{(2)} + \delta m_2 L_2\Pi^{(4a,1*)} - \delta m_2(L_2)^2\Pi^{(2*)} \\ & - \delta m_2\Pi^{(6F,1*)} + 2B_2L_{4a,1}\Pi^{(2)} + B_2L_2\Pi^{(4a)} - 2B_2(L_2)^2\Pi^{(2)} - B_2\Pi^{(6F)} - L_{6D,1}\Pi^{(2)} + L_{4b,1}L_2\Pi^{(2)} \\ & - L_{4a,1}\Pi^{(4b)} - L_2\Pi^{(6E)} + (L_2)^2\Pi^{(4b)},\end{aligned}$$

$$\begin{aligned}\Pi_{\rm ren}^{(p28)} = {} & \Pi^{(p28)} + \delta m_{4b}\delta m_2\Pi^{(2**)} + \delta m_{4b}B_2\Pi^{(2*)} - \delta m_{4b}\Pi^{(4b,1*)} - \delta m_{2*}\delta m_2 B_2\Pi^{(2*)} + \delta m_{2*}\delta m_2\Pi^{(4b,1*)} \\ & - \delta m_{2*}(\delta m_2)^2\Pi^{(2**)} + \delta m_2 B_{4b}\Pi^{(2*)} - \delta m_2 B_{2*}B_2\Pi^{(2)} + \delta m_2 B_{2*}\Pi^{(4b)} + \delta m_2 B_2\Pi^{(4b,2*)} + 2\delta m_2 B_2\Pi^{(4b,1*)} \\ & - 2\delta m_2(B_2)^2\Pi^{(2*)} - \delta m_2\Pi^{(6C,1*)} - \delta m_2\Pi^{(6A,2*)} - (\delta m_2)^2 B_{2*}\Pi^{(2*)} - (\delta m_2)^2 B_2\Pi^{(2**)} + (\delta m_2)^2\Pi^{(4b,1*2*)} \\ & + B_{4b}B_2\Pi^{(2)} - B_{4b}\Pi^{(4b)} - B_2\Pi^{(6C)} - B_2\Pi^{(6A)} + 2(B_2)^2\Pi^{(4b)} - (B_2)^3\Pi^{(2)},\end{aligned}$$

$$\Pi_{\rm ren}^{(p29)} = \Pi^{(p29)} + \delta m_2 L_{4a,2(2*)}\Pi^{(2)} + \delta m_2 L_{4a,2}\Pi^{(2*)} - \delta m_2 \Pi^{(6H,1*)} + 2B_2 L_{4a,2}\Pi^{(2)} - B_2\Pi^{(6H)} - L_{6E,2}\Pi^{(2)} - L_{4a,2}\Pi^{(4b)},$$

$$\Pi_{\rm ren}^{(p30)} = \Pi^{(p30)} + \delta m_2 L_{4b,2(2*)}\Pi^{(2)} + \delta m_2 L_{4b,2}\Pi^{(2*)} - 2\delta m_2 L_{2*}L_2\Pi^{(2)} + \delta m_2 L_{2*}\Pi^{(4a)} + \delta m_2 L_2 \Pi^{(4a,1*)} - \delta m_2 (L_2)^2\Pi^{(2*)} - \delta m_2\Pi^{(6G,1*)} + 2B_2 L_{4b,2}\Pi^{(2)} + 2B_2 L_2\Pi^{(4a)} - 3B_2(L_2)^2\Pi^{(2)} - B_2\Pi^{(6G)} - L_{6B,2}\Pi^{(2)} - L_{4b,2}\Pi^{(4b)} + 2L_{4b,1}L_2\Pi^{(2)} - L_{4b,1}\Pi^{(4a)} - L_2\Pi^{(6E)} + (L_2)^2\Pi^{(4b)},$$

$$\Pi_{\rm ren}^{(p31)} = \Pi^{(p31)} + \delta m_2 L_{4a,1(1*)}\Pi^{(2)} + \delta m_2 L_{4a,1}\Pi^{(2*)} - \delta m_2 L_{2*}L_2\Pi^{(2)} + \delta m_2 L_2\Pi^{(4a,1*)} - \delta m_2 (L_2)^2\Pi^{(2*)} - \delta m_2\Pi^{(6F,5*)} + 2B_2 L_{4a,1}\Pi^{(2)} + B_2 L_2\Pi^{(4a)} - 2B_2(L_2)^2\Pi^{(2)} - B_2\Pi^{(6F)} - L_{6D,3}\Pi^{(2)} + L_{4b,1}L_2\Pi^{(2)} - L_{4a,1}\Pi^{(4b)} - L_2\Pi^{(6E)} + (L_2)^2\Pi^{(4b)},$$

$$\Pi_{\rm ren}^{(p32)} = \Pi^{(p32)} + \delta m_{4a} L_{2*}\Pi^{(2)} + \delta m_{4a} L_2\Pi^{(2*)} - \delta m_{4a}\Pi^{(4a,1*)} - 2\delta m_2 L_{2*}L_2\Pi^{(2)} + 2\delta m_2 L_2\Pi^{(4a,1*)} - 2\delta m_2(L_2)^2\Pi^{(2*)} + 2B_{4a}L_2\Pi^{(2)} - B_{4a}\Pi^{(4a)} + 2B_2 L_2\Pi^{(4a)} - 4B_2(L_2)^2\Pi^{(2)} - L_{6C,1}\Pi^{(2)} + 2L_{4b,1}L_2\Pi^{(2)} - 2L_2\Pi^{(6E)} - L_2\Pi^{(6D)} + 2(L_2)^2\Pi^{(4b)},$$

$$\Pi_{\rm ren}^{(p33)} = \Pi^{(p33)} - L_{6G,1}\Pi^{(2)} - L_{6F,1}\Pi^{(2)} + 4L_{4a,1}L_2\Pi^{(2)} - L_{4a,1}\Pi^{(4a)} - L_2\Pi^{(6F)} + (L_2)^2\Pi^{(4a)} - 2(L_2)^3\Pi^{(2)},$$

$$\Pi_{\rm ren}^{(p34)} = \Pi^{(p34)} - \delta m_{6D}\Pi^{(2*)} + \delta m_{4b}L_2\Pi^{(2*)} + \delta m_{4a(1*)}\delta m_2\Pi^{(2*)} + \delta m_{4a}B_2\Pi^{(2*)} - \delta m_{2*}\delta m_2 L_2\Pi^{(2*)} + \delta m_2 B_{4a(1*)}\Pi^{(2)} - \delta m_2 B_{2*}L_2\Pi^{(2)} - \delta m_2 B_2 L_{2*}\Pi^{(2)} - 2\delta m_2 B_2 L_2\Pi^{(2*)} + \delta m_2 L_{4b,1}\Pi^{(2*)} + \delta m_2 L_{2*}\Pi^{(4b)} + \delta m_2 L_2\Pi^{(4b,2*)} - \delta m_2\Pi^{(6D,2*)} - (\delta m_2)^2 L_{2*}\Pi^{(2*)} - B_{6D}\Pi^{(2)} + B_{4b}L_2\Pi^{(2)} + B_{4a}B_2\Pi^{(2)} + B_2 L_{4b,1}\Pi^{(2)} + 2B_2 L_2\Pi^{(4b)} - B_2\Pi^{(6D)} - 2(B_2)^2 L_2\Pi^{(2)} - L_{4b,1}\Pi^{(4b)} - L_2\Pi^{(6C)},$$

$$\Pi_{\rm ren}^{(p35)} = \Pi^{(p35)} - L_{6G,4}\Pi^{(2)} - L_{6F,2}\Pi^{(2)} + 2L_{4a,2}L_2\Pi^{(2)} - L_2\Pi^{(6H)},$$

$$\Pi_{\rm ren}^{(p36)} = \Pi^{(p36)} - L_{6D,2}\Pi^{(2)} - L_{6C,2}\Pi^{(2)} + 2L_{4b,2}L_2\Pi^{(2)} + 3L_{4a,1}L_2\Pi^{(2)} - L_{4a,1}\Pi^{(4a)} - L_2\Pi^{(6G)} - L_2\Pi^{(6F)} + 2(L_2)^2\Pi^{(4a)} - 3(L_2)^3\Pi^{(2)},$$

$$\Pi_{\rm ren}^{(p37)} = \Pi^{(p37)} + \delta m_{4b}L_{2*}\Pi^{(2)} + \delta m_{4b}L_2\Pi^{(2*)} - \delta m_{4b}\Pi^{(4a,1*)} - \delta m_{2*}\delta m_2 L_{2*}\Pi^{(2)} - \delta m_{2*}\delta m_2 L_2\Pi^{(2*)} + \delta m_{2*}\delta m_2\Pi^{(4a,1*)} - 2\delta m_2 B_{2*}L_2\Pi^{(2)} + \delta m_2 B_{2*}\Pi^{(4a)} - \delta m_2 B_2 L_{2*}\Pi^{(2)} - \delta m_2 B_2 L_2\Pi^{(2*)} + \delta m_2 B_2\Pi^{(4a,1*)} + \delta m_2 L_{4b,1(3*)}\Pi^{(2)} + \delta m_2 L_2\Pi^{(4b,2*)} - \delta m_2\Pi^{(6E,3*)} + 2B_{4b}L_2\Pi^{(2)} - B_{4b}\Pi^{(4a)} + B_2 L_{4b,1}\Pi^{(2)} + B_2 L_2\Pi^{(4b)} - B_2\Pi^{(6E)} - 2(B_2)^2 L_2\Pi^{(2)} + (B_2)^2\Pi^{(4a)} - L_{6B,1}\Pi^{(2)} - L_2\Pi^{(6C)},$$

$$\Pi_{\rm ren}^{(p38)} = \Pi^{(p38)} + \delta m_2 L_{4a,1(4*)}\Pi^{(2)} + \delta m_2 L_{4a,1(3*)}\Pi^{(2)} - 2\delta m_2 L_{2*}L_2\Pi^{(2)} + \delta m_2 L_{2*}\Pi^{(4a)} - \delta m_2\Pi^{(6F,2*)} + 2B_2 L_{4a,1}\Pi^{(2)} + B_2 L_2\Pi^{(4a)} - 2B_2(L_2)^2\Pi^{(2)} - B_2\Pi^{(6F)} - L_{6E,1}\Pi^{(2)} - L_{6D,5}\Pi^{(2)} + 2L_{4b,1}L_2\Pi^{(2)} - L_{4b,1}\Pi^{(4a)},$$

$$\Pi_{\rm ren}^{(p39)} = \Pi^{(p39)} - \delta m_{6G}\Pi^{(2*)} + \delta m_{4a}L_2\Pi^{(2*)} + \delta m_2 L_{4b,2}\Pi^{(2*)} + \delta m_2 L_{4a,1}\Pi^{(2*)} - 2\delta m_2(L_2)^2\Pi^{(2*)} - B_{6G}\Pi^{(2)} + B_{4a}L_2\Pi^{(2)} + B_2 L_{4b,2}\Pi^{(2)} + B_2 L_{4a,1}\Pi^{(2)} - 2B_2(L_2)^2\Pi^{(2)} - L_{4b,2}\Pi^{(4b)} - L_{4a,1}\Pi^{(4b)} - L_2\Pi^{(6D)} + 2(L_2)^2\Pi^{(4b)}.$$

APPENDIX C: INTERMEDIATE RENORMALIZATION BY K OPERATION

This appendix describes how UV-divergent subdiagrams obtained by applying the K operation on the original unrenormalized vacuum-polarization functions are separated out.

$L_2^{\rm UV}$, $B_2^{\rm UV}$, etc., denote UV-divergent parts of renormalization constants L_2, B_2, etc., defined by the K operation. Quantities with Δ attached in front are *finite parts* of the quantities. Note that $\Delta\delta m_2 = 0$ so that $\delta m_2^{\rm UV}$ can be replaced by δm_2. Derivative amplitudes [25] are denoted as L_2', B_2', etc.

1. Fourth-order vacuum polarization

$$\Pi^{(4a)} = \Delta\Pi^{(4a)} + 2L_2^{\rm UV}\Pi^{(2)},$$

$$\Pi^{(4b)} = \Delta\Pi^{(4b)} + B_2^{\rm UV}\Pi^{(2)} + \delta m_2\Pi^{(2*)}.$$

2. Sixth-order vacuum polarization

$$\Pi^{(6A)} = \Delta\Pi^{(6A)} + 2B_2^{\rm UV}\Pi^{(4b)} - (B_2^{\rm UV})^2\Pi^{(2)} + 2\delta m_2\Pi^{(4b,1*)} - 2\delta m_2 B_2^{\rm UV}\Pi^{(2*)} - (\delta m_2)^2\Pi^{(2**)},$$

$$\Pi^{(6B)} = \Delta\Pi^{(6B)} + 2B_2^{\rm UV}\Pi^{(4b)} - (B_2^{\rm UV})^2\Pi^{(2)} + 2\delta m_2\Pi^{(4b,4*)} - 2\delta m_2 B_2^{\rm UV}\Pi^{(2*)} - (\delta m_2)^2\Pi^{(2**)},$$

$$\Pi^{(6C)} = \Delta\Pi^{(6C)} + B_2^{\rm UV}\Pi^{(4b)} - B_2^{\rm UV}B_2'^{\rm UV}\Pi^{(2)} + B_{4b}^{\rm UV}\Pi^{(2)} - \delta m_2'^{\rm UV}B_2^{\rm UV}\Pi^{(2*)} + \delta m_2\Pi^{(4b,2*)} - \delta m_2\delta m_{2*}^{\rm UV}\Pi^{(2*)} + \delta m_{4b}^{\rm UV}\Pi^{(2*)},$$

$$\Pi^{(6D)} = \Delta\Pi^{(6D)} + B_{4a}^{\rm UV}\Pi^{(2)} + 2L_2^{\rm UV}\Pi^{(4b)} - 2L_2^{\rm UV}B_2^{\rm UV}\Pi^{(2)} - 2\delta m_2 L_2^{\rm UV}\Pi^{(2*)} + \delta m_{4a}^{\rm UV}\Pi^{(2*)},$$

$$\Pi^{(6E)} = \Delta\Pi^{(6E)} + B_2^{\rm UV}\Pi^{(4a)} - L_2'^{\rm UV}B_2^{\rm UV}\Pi^{(2)} + L_2^{\rm UV}\Pi^{(4b)} - L_2^{\rm UV}B_2^{\rm UV}\Pi^{(2)} + L_{4b,1}^{\rm UV}\Pi^{(2)} + \delta m_2\Pi^{(4a,1*)} - \delta m_2 L_2^{\rm UV}\Pi^{(2*)},$$

$$\Pi^{(6F)} = \Delta\Pi^{(6F)} + L_2^{\rm UV}\Pi^{(4a)} - 2(L_2^{\rm UV})^2\Pi^{(2)} + 2L_{4a,1}^{\rm UV}\Pi^{(2)},$$

$$\Pi^{(6G)} = \Delta\Pi^{(6G)} + 2L_2^{\rm UV}\Pi^{(4a)} - 3(L_2^{\rm UV})^2\Pi^{(2)} + 2L_{4b,2}^{\rm UV}\Pi^{(2)},$$

$$\Pi^{(6H)} = \Delta\Pi^{(6H)} + 2L_{4a,2}^{\rm UV}\Pi^{(2)}.$$

3. Eighth-order vacuum polarization

$$\Pi^{(p01)} = \Delta\Pi^{(p01)} + 2L_2^{\rm UV}\Pi^{(6F)} - (L_2^{\rm UV})^2\Pi^{(4a)} + 2(L_2^{\rm UV})^3\Pi^{(2)} - 4L_{4a,1}^{\rm UV}L_2^{\rm UV}\Pi^{(2)} + 2L_{6F,3}^{\rm UV}\Pi^{(2)},$$

$$\Pi^{(p02)} = \Delta\Pi^{(p02)} + 2L_{6H,3}^{\rm UV}\Pi^{(2)},$$

$$\Pi^{(p03)} = \Delta\Pi^{(p03)} + 2L_2^{\rm UV}\Pi^{(6G)} - 3(L_2^{\rm UV})^2\Pi^{(4a)} + 4(L_2^{\rm UV})^3\Pi^{(2)} + 2L_{4b,2}^{\rm UV}\Pi^{(4a)} - 6L_{4b,2}^{\rm UV}L_2^{\rm UV}\Pi^{(2)} + 2L_{6B,3}^{\rm UV}\Pi^{(2)},$$

$$\Pi^{(p04)} = \Delta\Pi^{(p04)} + 3B_2^{\rm UV}\Pi^{(6A)} - 3(B_2^{\rm UV})^2\Pi^{(4b)} + (B_2^{\rm UV})^3\Pi^{(2)} + \delta m_2\Pi^{(6A,3*)} + 2\delta m_2\Pi^{(6A,1*)} - 6\delta m_2 B_2^{\rm UV}\Pi^{(4b,1*)} + 3\delta m_2(B_2^{\rm UV})^2\Pi^{(2*)} - (\delta m_2)^2\Pi^{(4b,1*3*)} - 2(\delta m_2)^2\Pi^{(4b,1*1*)} + 3(\delta m_2)^2 B_2^{\rm UV}\Pi^{(2**)} + (\delta m_2)^3\Pi^{(2***)},$$

$$\Pi^{(p05)} = \Delta\Pi^{(p05)} + 2B_2^{\rm UV}\Pi^{(6B)} + B_2^{\rm UV}\Pi^{(6A)} - 3(B_2^{\rm UV})^2\Pi^{(4b)} + (B_2^{\rm UV})^3\Pi^{(2)} + 2\delta m_2\Pi^{(6B,1*)} + \delta m_2\Pi^{(6A,6*)} - 4\delta m_2 B_2^{\rm UV}\Pi^{(4b,4*)} - 2\delta m_2 B_2^{\rm UV}\Pi^{(4b,1*)} + 3\delta m_2(B_2^{\rm UV})^2\Pi^{(2*)} - (\delta m_2)^2\Pi^{(4b,4*4*)} - 2(\delta m_2)^2\Pi^{(4b,1*4*)} + 2(\delta m_2)^2 B_2^{\rm UV}\Pi^{(2**)} + (\delta m_2)^2 B_2^{\rm UV}\Pi^{(2**)} + (\delta m_2)^3\Pi^{(2***)},$$

$$\Pi^{(p06)} = \Delta\Pi^{(p06)} + 2B_2^{\rm UV}\Pi^{(6E)} - (B_2^{\rm UV})^2\Pi^{(4a)} - L_2'^{\rm UV}B_2^{\rm UV}\Pi^{(4b)} + L_2'^{\rm UV}(B_2^{\rm UV})^2\Pi^{(2)} - L_2'^{\rm UV}B_2^{\rm UV}\Pi^{(4b)} + L_2'^{\rm UV}(B_2^{\rm UV})^2\Pi^{(2)} + 2L_{4b,1}^{\rm UV}\Pi^{(4b)} - 2L_{4b,1}^{\rm UV}B_2^{\rm UV}\Pi^{(2)} + 2\delta m_2\Pi^{(6E,1*)} - 2\delta m_2 B_2^{\rm UV}\Pi^{(4a,1*)} + \delta m_2 L_2'^{\rm UV}B_2^{\rm UV}\Pi^{(2*)} + \delta m_2 L_2'^{\rm UV}B_2^{\rm UV}\Pi^{(2*)} - 2\delta m_2 L_{4b,1}^{\rm UV}\Pi^{(2*)} - (\delta m_2)^2\Pi^{(4a,1*2*)},$$

$$\Pi^{(p07)} = \Delta\Pi^{(p07)} + 2B_2^{\rm UV}\Pi^{(6E)} - (B_2^{\rm UV})^2\Pi^{(4a)} + L_2''^{\rm UV}(B_2^{\rm UV})^2\Pi^{(2)} + L_2^{\rm UV}\Pi^{(6B)} - 2L_2^{\rm UV}B_2^{\rm UV}\Pi^{(4b)} + L_2^{\rm UV}(B_2^{\rm UV})^2\Pi^{(2)} - 2L_{4b,1(1')}^{\rm UV}B_2^{\rm UV}\Pi^{(2)} + L_{6A,3}^{\rm UV}\Pi^{(2)} + 2\delta m_2\Pi^{(6E,5*)} - 2\delta m_2 B_2^{\rm UV}\Pi^{(4a,1*)} - 2\delta m_2 L_2^{\rm UV}\Pi^{(4b,4*)} + 2\delta m_2 L_2^{\rm UV}B_2^{\rm UV}\Pi^{(2*)} - (\delta m_2)^2\Pi^{(4a,1*4*)} + (\delta m_2)^2 L_2^{\rm UV}\Pi^{(2**)},$$

$$\Pi^{(p08)} = \Delta\Pi^{(p08)} + 2B_2^{\rm UV}\Pi^{(6E)} - (B_2^{\rm UV})^2\Pi^{(4a)} - 2L_2'^{\rm UV}B_2^{\rm UV}\Pi^{(4b)} + 2L_2'^{\rm UV}(B_2^{\rm UV})^2\Pi^{(2)} + 2L_{4b,1}^{\rm UV}\Pi^{(4b)} - 2L_{4b,1}^{\rm UV}B_2^{\rm UV}\Pi^{(2)} + 2\delta m_2\Pi^{(6E,6*)} - 2\delta m_2 B_2^{\rm UV}\Pi^{(4a,1*)} + 2\delta m_2 L_2'^{\rm UV}B_2^{\rm UV}\Pi^{(2*)} - 2\delta m_2 L_{4b,1}^{\rm UV}\Pi^{(2*)} - (\delta m_2)^2\Pi^{(4a,1*3*)},$$

$$\Pi^{(p09)} = \Delta\Pi^{(p09)} + B_2^{\rm UV}\Pi^{(6D)} + B_{4a}^{\rm UV}\Pi^{(4b)} - B_{4a}^{\rm UV}B_2^{\rm UV}\Pi^{(2)} + 2L_2^{\rm UV}\Pi^{(6B)} - 4L_2^{\rm UV}B_2^{\rm UV}\Pi^{(4b)} + 2L_2^{\rm UV}(B_2^{\rm UV})^2\Pi^{(2)} + \delta m_2\Pi^{(6D,6*)} - \delta m_2 B_{4a}^{\rm UV}\Pi^{(2*)} - 4\delta m_2 L_2^{\rm UV}\Pi^{(4b,4*)} + 4\delta m_2 L_2^{\rm UV}B_2^{\rm UV}\Pi^{(2*)} + 2(\delta m_2)^2 L_2^{\rm UV}\Pi^{(2**)} + \delta m_{4a}^{\rm UV}\Pi^{(4b,4*)} - \delta m_{4a}^{\rm UV}B_2^{\rm UV}\Pi^{(2*)} - \delta m_{4a}^{\rm UV}\delta m_2\Pi^{(2**)},$$

$$\Pi^{(p10)} = \Delta\Pi^{(p10)} + B_2^{\rm UV}\Pi^{(6C)} + B_2^{\rm UV}\Pi^{(6B)} - B_2^{\rm UV}B_2'^{\rm UV}\Pi^{(4b)} - (B_2^{\rm UV})^2\Pi^{(4b)} + (B_2^{\rm UV})^2B_2'^{\rm UV}\Pi^{(2)} + B_{4b}^{\rm UV}\Pi^{(4b)} - B_{4b}^{\rm UV}B_2^{\rm UV}\Pi^{(2)} - \delta m_2'^{\rm UV}B_2^{\rm UV}\Pi^{(4b,4*)} + \delta m_2'^{\rm UV}(B_2^{\rm UV})^2\Pi^{(2*)} + \delta m_2\Pi^{(6C,6*)} + \delta m_2\Pi^{(6B,2*)} - \delta m_2 B_2^{\rm UV}\Pi^{(4b,4*)} - \delta m_2 B_2^{\rm UV}\Pi^{(4b,2*)} + \delta m_2 B_2^{\rm UV}B_2'^{\rm UV}\Pi^{(2*)} - \delta m_2 B_{4b}^{\rm UV}\Pi^{(2*)} - \delta m_2\delta m_{2*}^{\rm UV}\Pi^{(4b,4*)} + \delta m_2\delta m_{2*}^{\rm UV}B_2^{\rm UV}\Pi^{(2*)} + \delta m_2\delta m_2'^{\rm UV}B_2^{\rm UV}\Pi^{(2**)} - (\delta m_2)^2\Pi^{(4b,2*4*)} + (\delta m_2)^2\delta m_{2*}^{\rm UV}\Pi^{(2**)} + \delta m_{4b}^{\rm UV}\Pi^{(4b,4*)} - \delta m_{4b}^{\rm UV}B_2^{\rm UV}\Pi^{(2*)} - \delta m_{4b}^{\rm UV}\delta m_2\Pi^{(2**)},$$

$$\Pi^{(p11)} = \Delta\Pi^{(p11)} + B_{6F}^{\rm UV}\Pi^{(2)} + 2L_2^{\rm UV}\Pi^{(6D)} - 2L_2^{\rm UV}B_{4a}^{\rm UV}\Pi^{(2)} - 3(L_2^{\rm UV})^2\Pi^{(4b)} + 3(L_2^{\rm UV})^2B_2^{\rm UV}\Pi^{(2)} + 2L_{4a,1}^{\rm UV}\Pi^{(4b)} - 2L_{4a,1}^{\rm UV}B_2^{\rm UV}\Pi^{(2)} + 3\delta m_2(L_2^{\rm UV})^2\Pi^{(2*)} - 2\delta m_2 L_{4a,1}^{\rm UV}\Pi^{(2*)} - 2\delta m_{4a}^{\rm UV}L_2^{\rm UV}\Pi^{(2*)} + \delta m_{6F}^{\rm UV}\Pi^{(2*)},$$

$$\Pi^{(p12)} = \Delta\Pi^{(p12)} + 2B_2^{\rm UV}\Pi^{(6C)} - (B_2^{\rm UV})^2\Pi^{(4b)} + (B_2^{\rm UV})^2B_2''^{\rm UV}\Pi^{(2)} - B_{4b(3')}^{\rm UV}B_2^{\rm UV}\Pi^{(2)} - B_{4b(1')}^{\rm UV}B_2^{\rm UV}\Pi^{(2)} + B_{6A}^{\rm UV}\Pi^{(2)} + \delta m_2''^{\rm UV}(B_2^{\rm UV})^2\Pi^{(2*)} + 2\delta m_2\Pi^{(6C,2*)} - 2\delta m_2 B_2^{\rm UV}\Pi^{(4b,2*)} + \delta m_2\delta m_{2*}'^{\rm UV}B_2^{\rm UV}\Pi^{(2*)} + \delta m_2\delta m_{2*}'^{\rm UV}B_2^{\rm UV}\Pi^{(2*)} - (\delta m_2)^2\Pi^{(4b,2*2*)} + (\delta m_2)^2\delta m_{2**}^{\rm UV}\Pi^{(2*)} - 2\delta m_{4b(1*)}^{\rm UV}\delta m_2\Pi^{(2*)} - \delta m_{4b(3')}^{\rm UV}B_2^{\rm UV}\Pi^{(2*)} - \delta m_{4b(1')}^{\rm UV}B_2^{\rm UV}\Pi^{(2*)} + \delta m_{6A}^{\rm UV}\Pi^{(2*)},$$

$$\Pi^{(p13)} = \Delta\Pi^{(p13)} + B_2^{\rm UV}\Pi^{(6H)} - L_{4a,2(4')}^{\rm UV}B_2^{\rm UV}\Pi^{(2)} - L_{4a,2(1')}^{\rm UV}B_2^{\rm UV}\Pi^{(2)} + 2L_{6D,4}^{\rm UV}\Pi^{(2)} + \delta m_2\Pi^{(6H,2*)},$$

$$\Pi^{(p14)} = \Delta\Pi^{(p14)} + B_2^{\rm UV}\Pi^{(6G)} + 2L_2^{\rm UV}\Pi^{(6E)} - 2L_2^{\rm UV}B_2^{\rm UV}\Pi^{(4a)} + L_2^{\rm UV}L_2'^{\rm UV}B_2^{\rm UV}\Pi^{(2)} + L_2^{\rm UV}L_2'^{\rm UV}B_2^{\rm UV}\Pi^{(2)} - (L_2^{\rm UV})^2\Pi^{(4b)} + (L_2^{\rm UV})^2B_2^{\rm UV}\Pi^{(2)} - L_{4b,2(4')}^{\rm UV}B_2^{\rm UV}\Pi^{(2)} - L_{4b,2(1')}^{\rm UV}B_2^{\rm UV}\Pi^{(2)} - 2L_{4b,1}^{\rm UV}L_2^{\rm UV}\Pi^{(2)} + 2L_{6A,2}^{\rm UV}\Pi^{(2)} + \delta m_2\Pi^{(6G,2*)} - 2\delta m_2 L_2^{\rm UV}\Pi^{(4a,1*)} + \delta m_2(L_2^{\rm UV})^2\Pi^{(2*)},$$

$$\Pi^{(p15)} = \Delta\Pi^{(p15)} + B_{6H}^{\rm UV}\Pi^{(2)} + 2L_{4a,2}^{\rm UV}\Pi^{(4b)} - 2L_{4a,2}^{\rm UV}B_2^{\rm UV}\Pi^{(2)} - 2\delta m_2 L_{4a,2}^{\rm UV}\Pi^{(2*)} + \delta m_{6H}^{\rm UV}\Pi^{(2*)},$$

$$\Pi^{(p16)} = \Delta\Pi^{(p16)} + L_{4a,2}^{\rm UV}\Pi^{(4a)} - 2L_{4a,2}^{\rm UV}L_2^{\rm UV}\Pi^{(2)} + 2L_{6H,1}^{\rm UV}\Pi^{(2)},$$

$$\Pi^{(p17)} = \Delta\Pi^{(p17)} + 2L_{6H,2}^{\rm UV}\Pi^{(2)},$$

$$\Pi^{(p18)} = \Delta\Pi^{(p18)} + 2L_{6G,2}^{\rm UV}\Pi^{(2)},$$

$$\Pi^{(p19)} = \Delta\Pi^{(p19)} + L_2^{\rm UV}\Pi^{(6F)} - (L_2^{\rm UV})^2\Pi^{(4a)} + 2(L_2^{\rm UV})^3\Pi^{(2)} + L_{4b,2}^{\rm UV}\Pi^{(4a)} - 2L_{4b,2}^{\rm UV}L_2^{\rm UV}\Pi^{(2)} - 2L_{4a,1}^{\rm UV}L_2^{\rm UV}\Pi^{(2)} + 2L_{6G,5}^{\rm UV}\Pi^{(2)},$$

$$\Pi^{(p20)} = \Delta\Pi^{(p20)} + B_{4a}^{\rm UV}\Pi^{(4b)} - B_{4a}^{\rm UV}B_2'^{\rm UV}\Pi^{(2)} + B_{6C}^{\rm UV}\Pi^{(2)} + 2L_2^{\rm UV}\Pi^{(6C)} - 2L_2^{\rm UV}B_2^{\rm UV}\Pi^{(4b)} + 2L_2^{\rm UV}B_2^{\rm UV}B_2'^{\rm UV}\Pi^{(2)} - 2L_2^{\rm UV}B_{4b}^{\rm UV}\Pi^{(2)} - \delta m_2'^{\rm UV}B_{4a}^{\rm UV}\Pi^{(2*)} + 2\delta m_2'^{\rm UV}L_2^{\rm UV}B_2^{\rm UV}\Pi^{(2*)} - 2\delta m_2 L_2^{\rm UV}\Pi^{(4b,2*)} + 2\delta m_2\delta m_{2*}^{\rm UV}L_2^{\rm UV}\Pi^{(2*)} - 2\delta m_{4b}^{\rm UV}L_2^{\rm UV}\Pi^{(2*)} + \delta m_{4a}^{\rm UV}\Pi^{(4b,2*)} - \delta m_{4a}^{\rm UV}\delta m_{2*}^{\rm UV}\Pi^{(2*)} + \delta m_{6C}^{\rm UV}\Pi^{(2*)},$$

$$\Pi^{(p21)} = \Delta\Pi^{(p21)} + B_2^{\rm UV}\Pi^{(6D)} - B_{4a(2')}^{\rm UV}B_2^{\rm UV}\Pi^{(2)} + B_{6E}^{\rm UV}\Pi^{(2)} - L_2^{\prime\rm UV}B_2^{\rm UV}\Pi^{(4b)} + L_2^{\prime\rm UV}(B_2^{\rm UV})^2\Pi^{(2)} - L_2^{\prime\rm UV}B_2^{\rm UV}\Pi^{(4b)} + L_2^{\prime\rm UV}(B_2^{\rm UV})^2\Pi^{(2)} + 2L_{4b,1}^{\rm UV}\Pi^{(4b)} - 2L_{4b,1}^{\rm UV}B_2^{\rm UV}\Pi^{(2)} + \delta m_2\Pi^{(6D,3*)} + \delta m_2 L_2^{\prime\rm UV}B_2^{\rm UV}\Pi^{(2*)} + \delta m_2 L_2^{\prime\rm UV}B_2^{\rm UV}\Pi^{(2*)} - 2\delta m_2 L_{4b,1}^{\rm UV}\Pi^{(2*)} - \delta m_{4a(2*)}^{\rm UV}\delta m_2\Pi^{(2*)} - \delta m_{4a(2')}^{\rm UV}B_2^{\rm UV}\Pi^{(2*)} + \delta m_{6E}^{\rm UV}\Pi^{(2*)},$$

$$\Pi^{(p22)} = \Delta\Pi^{(p22)} + B_2^{\rm UV}\Pi^{(6C)} - B_2^{\rm UV}B_2^{\prime\rm UV}\Pi^{(4b)} + B_2^{\rm UV}(B_2^{\prime\rm UV})^2\Pi^{(2)} - B_{4b(2')}^{\rm UV}B_2^{\rm UV}\Pi^{(2)} + B_{4b}^{\rm UV}\Pi^{(4b)} - B_{4b}^{\rm UV}B_2^{\prime\rm UV}\Pi^{(2)} + B_{6B}^{\rm UV}\Pi^{(2)} - \delta m_2^{\prime\rm UV}B_2^{\rm UV}\Pi^{(4b,2*)} + \delta m_2^{\prime\rm UV}B_2^{\rm UV}B_2^{\prime\rm UV}\Pi^{(2*)} - \delta m_2^{\prime\rm UV}B_{4b}^{\rm UV}\Pi^{(2*)} + \delta m_2^{\prime\rm UV}\delta m_{2*}^{\rm UV}B_2^{\rm UV}\Pi^{(2*)} + \delta m_2\Pi^{(6C,3*)} - \delta m_2\delta m_{2*}^{\rm UV}\Pi^{(4b,2*)} + \delta m_2(\delta m_{2*}^{\rm UV})^2\Pi^{(2*)} - \delta m_{4b(2*)}^{\rm UV}\delta m_2\Pi^{(2*)} - \delta m_{4b(2')}^{\rm UV}B_2^{\rm UV}\Pi^{(2*)} + \delta m_{4b}^{\rm UV}\Pi^{(4b,2*)} - \delta m_{4b}^{\rm UV}\delta m_{2*}^{\rm UV}\Pi^{(2*)} + \delta m_{6B}^{\rm UV}\Pi^{(2*)},$$

$$\Pi^{(p23)} = \Delta\Pi^{(p23)} + 2L_{6G,3}^{\rm UV}\Pi^{(2)},$$

$$\Pi^{(p24)} = \Delta\Pi^{(p24)} + L_2^{\rm UV}\Pi^{(6H)} + L_{4a,2}^{\rm UV}\Pi^{(4a)} - 3L_{4a,2}^{\rm UV}L_2^{\rm UV}\Pi^{(2)} + L_{6E,3}^{\rm UV}\Pi^{(2)} + L_{6C,3}^{\rm UV}\Pi^{(2)},$$

$$\Pi^{(p25)} = \Delta\Pi^{(p25)} + 2B_2^{\rm UV}\Pi^{(6E)} - (B_2^{\rm UV})^2\Pi^{(4a)} + L_2^{\prime\prime\rm UV}(B_2^{\rm UV})^2\Pi^{(2)} + L_2^{\rm UV}\Pi^{(6A)} - 2L_2^{\rm UV}B_2^{\rm UV}\Pi^{(4b)} + L_2^{\rm UV}(B_2^{\rm UV})^2\Pi^{(2)} - L_{4b,1(4')}^{\rm UV}B_2^{\rm UV}\Pi^{(2)} - L_{4b,1(2')}^{\rm UV}B_2^{\rm UV}\Pi^{(2)} + L_{6A,1}^{\rm UV}\Pi^{(2)} + \delta m_2\Pi^{(6E,4*)} + \delta m_2\Pi^{(6E,2*)} - 2\delta m_2 B_2^{\rm UV}\Pi^{(4a,1*)} - 2\delta m_2 L_2^{\rm UV}\Pi^{(4b,1*)} + 2\delta m_2 L_2^{\rm UV}B_2^{\rm UV}\Pi^{(2*)} - (\delta m_2)^2\Pi^{(4a,1*1*)} + (\delta m_2)^2 L_2^{\rm UV}\Pi^{(2**)},$$

$$\Pi^{(p26)} = \Delta\Pi^{(p26)} + B_2^{\rm UV}\Pi^{(6D)} + B_{4a}^{\rm UV}\Pi^{(4b)} - B_{4a}^{\rm UV}B_2^{\rm UV}\Pi^{(2)} + 2L_2^{\rm UV}\Pi^{(6A)} - 4L_2^{\rm UV}B_2^{\rm UV}\Pi^{(4b)} + 2L_2^{\rm UV}(B_2^{\rm UV})^2\Pi^{(2)} + \delta m_2\Pi^{(6D,1*)} - \delta m_2 B_{4a}^{\rm UV}\Pi^{(2*)} - 4\delta m_2 L_2^{\rm UV}\Pi^{(4b,1*)} + 4\delta m_2 L_2^{\rm UV}B_2^{\rm UV}\Pi^{(2*)} + 2(\delta m_2)^2 L_2^{\rm UV}\Pi^{(2**)} + \delta m_{4a}^{\rm UV}\Pi^{(4b,1*)} - \delta m_{4a}^{\rm UV}B_2^{\rm UV}\Pi^{(2*)} - \delta m_{4a}^{\rm UV}\delta m_2\Pi^{(2**)},$$

$$\Pi^{(p27)} = \Delta\Pi^{(p27)} + B_2^{\rm UV}\Pi^{(6F)} + L_2^{\rm UV}\Pi^{(6E)} - L_2^{\rm UV}B_2^{\rm UV}\Pi^{(4a)} + L_2^{\rm UV}L_2^{\prime\rm UV}B_2^{\rm UV}\Pi^{(2)} - (L_2^{\rm UV})^2\Pi^{(4b)} + (L_2^{\rm UV})^2B_2^{\rm UV}\Pi^{(2)} - L_{4b,1}^{\rm UV}L_2^{\rm UV}\Pi^{(2)} - L_{4a,1(2')}^{\rm UV}B_2^{\rm UV}\Pi^{(2)} + L_{4a,1}^{\rm UV}\Pi^{(4b)} - L_{4a,1}^{\rm UV}B_2^{\rm UV}\Pi^{(2)} + L_{6D,1}^{\rm UV}\Pi^{(2)} + \delta m_2\Pi^{(6F,1*)} - \delta m_2 L_2^{\rm UV}\Pi^{(4a,1*)} + \delta m_2(L_2^{\rm UV})^2\Pi^{(2*)} - \delta m_2 L_{4a,1}^{\rm UV}\Pi^{(2*)},$$

$$\Pi^{(p28)} = \Delta\Pi^{(p28)} + B_2^{\rm UV}\Pi^{(6C)} + B_2^{\rm UV}\Pi^{(6A)} - B_2^{\rm UV}B_2^{\prime\rm UV}\Pi^{(4b)} - (B_2^{\rm UV})^2\Pi^{(4b)} + (B_2^{\rm UV})^2B_2^{\prime\rm UV}\Pi^{(2)} + B_{4b}^{\rm UV}\Pi^{(4b)} - B_{4b}^{\rm UV}B_2^{\rm UV}\Pi^{(2)} - \delta m_2^{\prime\rm UV}B_2^{\rm UV}\Pi^{(4b,1*)} + \delta m_2^{\prime\rm UV}(B_2^{\rm UV})^2\Pi^{(2*)} + \delta m_2\Pi^{(6C,1*)} + \delta m_2\Pi^{(6A,2*)} - \delta m_2 B_2^{\rm UV}\Pi^{(4b,2*)} - \delta m_2 B_2^{\rm UV}\Pi^{(4b,1*)} + \delta m_2 B_2^{\rm UV}B_2^{\prime\rm UV}\Pi^{(2*)} - \delta m_2 B_{4b}^{\rm UV}\Pi^{(2*)} - \delta m_2\delta m_{2*}^{\rm UV}\Pi^{(4b,1*)} + \delta m_2\delta m_{2*}^{\rm UV}B_2^{\rm UV}\Pi^{(2*)} + \delta m_2\delta m_2^{\prime\rm UV}B_2^{\rm UV}\Pi^{(2**)} - (\delta m_2)^2\Pi^{(4b,1*2*)} + (\delta m_2)^2\delta m_{2*}^{\rm UV}\Pi^{(2**)} + \delta m_{4b}^{\rm UV}\Pi^{(4b,1*)} - \delta m_{4b}^{\rm UV}B_2^{\rm UV}\Pi^{(2*)} - \delta m_{4b}^{\rm UV}\delta m_2\Pi^{(2**)},$$

$$\Pi^{(p29)} = \Delta\Pi^{(p29)} + B_2^{\rm UV}\Pi^{(6H)} - L_{4a,2(3')}^{\rm UV}B_2^{\rm UV}\Pi^{(2)} + L_{4a,2}^{\rm UV}\Pi^{(4b)} - L_{4a,2}^{\rm UV}B_2^{\rm UV}\Pi^{(2)} + L_{6E,2}^{\rm UV}\Pi^{(2)} + \delta m_2\Pi^{(6H,1*)} - \delta m_2 L_{4a,2}^{\rm UV}\Pi^{(2*)},$$

$$\Pi^{(p30)} = \Delta\Pi^{(p30)} + B_2^{\rm UV}\Pi^{(6G)} - L_2^{\prime\rm UV}B_2^{\rm UV}\Pi^{(4a)} + L_2^{\rm UV}\Pi^{(6E)} - L_2^{\rm UV}B_2^{\rm UV}\Pi^{(4a)} + 2L_2^{\rm UV}L_2^{\prime\rm UV}B_2^{\rm UV}\Pi^{(2)} - (L_2^{\rm UV})^2\Pi^{(4b)} + (L_2^{\rm UV})^2B_2^{\rm UV}\Pi^{(2)} - L_{4b,2(3')}^{\rm UV}B_2^{\rm UV}\Pi^{(2)} + L_{4b,2}^{\rm UV}\Pi^{(4b)} - L_{4b,2}^{\rm UV}B_2^{\rm UV}\Pi^{(2)} + L_{4b,1}^{\rm UV}\Pi^{(4a)} - 2L_{4b,1}^{\rm UV}L_2^{\rm UV}\Pi^{(2)} + L_{6B,2}^{\rm UV}\Pi^{(2)} + \delta m_2\Pi^{(6G,1*)} - \delta m_2 L_2^{\rm UV}\Pi^{(4a,1*)} + \delta m_2(L_2^{\rm UV})^2\Pi^{(2*)} - \delta m_2 L_{4b,2}^{\rm UV}\Pi^{(2*)},$$

$$\Pi^{(p31)} = \Delta\Pi^{(p31)} + B_2^{\mathrm{UV}}\Pi^{(6F)} + L_2^{\mathrm{UV}}\Pi^{(6E)} - L_2^{\mathrm{UV}}B_2^{\mathrm{UV}}\Pi^{(4a)} + L_2^{\mathrm{UV}}L_2'^{\mathrm{UV}}B_2^{\mathrm{UV}}\Pi^{(2)} - (L_2^{\mathrm{UV}})^2\Pi^{(4b)} + (L_2^{\mathrm{UV}})^2B_2^{\mathrm{UV}}\Pi^{(2)}$$
$$- L_{4b,1}^{\mathrm{UV}}L_2^{\mathrm{UV}}\Pi^{(2)} - L_{4a,1(1')}^{\mathrm{UV}}B_2^{\mathrm{UV}}\Pi^{(2)} + L_{4a,1}^{\mathrm{UV}}\Pi^{(4b)} - L_{4a,1}^{\mathrm{UV}}B_2^{\mathrm{UV}}\Pi^{(2)} + L_{6D,3}^{\mathrm{UV}}\Pi^{(2)} + \delta m_2\Pi^{(6F,5*)}$$
$$- \delta m_2 L_2^{\mathrm{UV}}\Pi^{(4a,1*)} + \delta m_2(L_2^{\mathrm{UV}})^2\Pi^{(2*)} - \delta m_2 L_{4a,1}^{\mathrm{UV}}\Pi^{(2*)},$$

$$\Pi^{(p32)} = \Delta\Pi^{(p32)} + B_{4a}^{\mathrm{UV}}\Pi^{(4a)} - L_2'^{\mathrm{UV}}B_{4a}^{\mathrm{UV}}\Pi^{(2)} + 2L_2^{\mathrm{UV}}\Pi^{(6E)} + L_2^{\mathrm{UV}}\Pi^{(6D)} - 2L_2^{\mathrm{UV}}B_2^{\mathrm{UV}}\Pi^{(4a)} - L_2^{\mathrm{UV}}B_{4a}^{\mathrm{UV}}\Pi^{(2)}$$
$$+ 2L_2^{\mathrm{UV}}L_2'^{\mathrm{UV}}B_2^{\mathrm{UV}}\Pi^{(2)} - 2(L_2^{\mathrm{UV}})^2\Pi^{(4b)} + 2(L_2^{\mathrm{UV}})^2B_2^{\mathrm{UV}}\Pi^{(2)} - 2L_{4b,1}^{\mathrm{UV}}L_2^{\mathrm{UV}}\Pi^{(2)} + L_{6C,1}^{\mathrm{UV}}\Pi^{(2)} - 2\delta m_2 L_2^{\mathrm{UV}}\Pi^{(4a,1*)}$$
$$+ 2\delta m_2(L_2^{\mathrm{UV}})^2\Pi^{(2*)} + \delta m_{4a}^{\mathrm{UV}}\Pi^{(4a,1*)} - \delta m_{4a}^{\mathrm{UV}}L_2^{\mathrm{UV}}\Pi^{(2*)},$$

$$\Pi^{(p33)} = \Delta\Pi^{(p33)} + L_2^{\mathrm{UV}}\Pi^{(6F)} - (L_2^{\mathrm{UV}})^2\Pi^{(4a)} + 2(L_2^{\mathrm{UV}})^3\Pi^{(2)} + L_{4a,1}^{\mathrm{UV}}\Pi^{(4a)} - 4L_{4a,1}^{\mathrm{UV}}L_2^{\mathrm{UV}}\Pi^{(2)} + L_{6G,1}^{\mathrm{UV}}\Pi^{(2)} + L_{6F,1}^{\mathrm{UV}}\Pi^{(2)},$$

$$\Pi^{(p34)} = \Delta\Pi^{(p34)} + B_2^{\mathrm{UV}}\Pi^{(6D)} - B_{4a(3')}^{\mathrm{UV}}B_2^{\mathrm{UV}}\Pi^{(2)} + B_{6D}^{\mathrm{UV}}\Pi^{(2)} - L_2'^{\mathrm{UV}}B_2^{\mathrm{UV}}\Pi^{(4b)} + L_2'^{\mathrm{UV}}(B_2^{\mathrm{UV}})^2\Pi^{(2)} + L_2^{\mathrm{UV}}\Pi^{(6C)}$$
$$- L_2^{\mathrm{UV}}B_2^{\mathrm{UV}}\Pi^{(4b)} + L_2^{\mathrm{UV}}B_2^{\mathrm{UV}}B_2'^{\mathrm{UV}}\Pi^{(2)} - L_2^{\mathrm{UV}}B_{4b}^{\mathrm{UV}}\Pi^{(2)} + L_{4b,1}^{\mathrm{UV}}\Pi^{(4b)} - L_{4b,1}^{\mathrm{UV}}B_2^{\mathrm{UV}}\Pi^{(2)} + \delta m_2'^{\mathrm{UV}}L_2^{\mathrm{UV}}B_2^{\mathrm{UV}}\Pi^{(2*)}$$
$$+ \delta m_2\Pi^{(6D,2*)} + \delta m_2 L_2'^{\mathrm{UV}}B_2^{\mathrm{UV}}\Pi^{(2*)} - \delta m_2 L_2^{\mathrm{UV}}\Pi^{(4b,2*)} - \delta m_2 L_{4b,1}^{\mathrm{UV}}\Pi^{(2*)} + \delta m_2\delta m_{2*}^{\mathrm{UV}}L_2^{\mathrm{UV}}\Pi^{(2*)}$$
$$- \delta m_{4b}^{\mathrm{UV}}L_2^{\mathrm{UV}}\Pi^{(2*)} - \delta m_{4a(1*)}^{\mathrm{UV}}\delta m_2\Pi^{(2*)} - \delta m_{4a(3')}^{\mathrm{UV}}B_2^{\mathrm{UV}}\Pi^{(2*)} + \delta m_{6D}^{\mathrm{UV}}\Pi^{(2*)},$$

$$\Pi^{(p35)} = \Delta\Pi^{(p35)} + L_2^{\mathrm{UV}}\Pi^{(6H)} - 2L_{4a,2}^{\mathrm{UV}}L_2^{\mathrm{UV}}\Pi^{(2)} + L_{6G,4}^{\mathrm{UV}}\Pi^{(2)} + L_{6F,2}^{\mathrm{UV}}\Pi^{(2)},$$

$$\Pi^{(p36)} = \Delta\Pi^{(p36)} + L_2^{\mathrm{UV}}\Pi^{(6G)} + L_2^{\mathrm{UV}}\Pi^{(6F)} - 2(L_2^{\mathrm{UV}})^2\Pi^{(4a)} + 3(L_2^{\mathrm{UV}})^3\Pi^{(2)} - 2L_{4b,2}^{\mathrm{UV}}L_2^{\mathrm{UV}}\Pi^{(2)} + L_{4a,1}^{\mathrm{UV}}\Pi^{(4a)}$$
$$- 3L_{4a,1}^{\mathrm{UV}}L_2^{\mathrm{UV}}\Pi^{(2)} + L_{6D,2}^{\mathrm{UV}}\Pi^{(2)} + L_{6C,2}^{\mathrm{UV}}\Pi^{(2)},$$

$$\Pi^{(p37)} = \Delta\Pi^{(p37)} + B_2^{\mathrm{UV}}\Pi^{(6E)} - B_2^{\mathrm{UV}}B_2'^{\mathrm{UV}}\Pi^{(4a)} + B_{4b}^{\mathrm{UV}}\Pi^{(4a)} + L_2'^{\mathrm{UV}}B_2^{\mathrm{UV}}B_2'^{\mathrm{UV}}\Pi^{(2)} - L_2'^{\mathrm{UV}}B_{4b}^{\mathrm{UV}}\Pi^{(2)} + L_2^{\mathrm{UV}}\Pi^{(6C)}$$
$$- L_2^{\mathrm{UV}}B_2^{\mathrm{UV}}\Pi^{(4b)} + L_2^{\mathrm{UV}}B_2^{\mathrm{UV}}B_2'^{\mathrm{UV}}\Pi^{(2)} - L_2^{\mathrm{UV}}B_{4b}^{\mathrm{UV}}\Pi^{(2)} - L_{4b,1(3')}^{\mathrm{UV}}B_2^{\mathrm{UV}}\Pi^{(2)} + L_{6B,1}^{\mathrm{UV}}\Pi^{(2)} - \delta m_2'^{\mathrm{UV}}B_2^{\mathrm{UV}}\Pi^{(4a,1*)}$$
$$+ \delta m_2'^{\mathrm{UV}}L_2^{\mathrm{UV}}B_2^{\mathrm{UV}}\Pi^{(2*)} + \delta m_2\Pi^{(6E,3*)} - \delta m_2 L_2^{\mathrm{UV}}\Pi^{(4b,2*)} - \delta m_2\delta m_{2*}^{\mathrm{UV}}\Pi^{(4a,1*)} + \delta m_2\delta m_{2*}^{\mathrm{UV}}L_2^{\mathrm{UV}}\Pi^{(2*)}$$
$$+ \delta m_{4b}^{\mathrm{UV}}\Pi^{(4a,1*)} - \delta m_{4b}^{\mathrm{UV}}L_2^{\mathrm{UV}}\Pi^{(2*)},$$

$$\Pi^{(p38)} = \Delta\Pi^{(p38)} + B_2^{\mathrm{UV}}\Pi^{(6F)} - L_2'^{\mathrm{UV}}B_2^{\mathrm{UV}}\Pi^{(4a)} + 2L_2^{\mathrm{UV}}L_2'^{\mathrm{UV}}B_2^{\mathrm{UV}}\Pi^{(2)} + L_{4b,1}^{\mathrm{UV}}\Pi^{(4a)} - 2L_{4b,1}^{\mathrm{UV}}L_2^{\mathrm{UV}}\Pi^{(2)}$$
$$- L_{4a,1(4')}^{\mathrm{UV}}B_2^{\mathrm{UV}}\Pi^{(2)} - L_{4a,1(3')}^{\mathrm{UV}}B_2^{\mathrm{UV}}\Pi^{(2)} + L_{6E,1}^{\mathrm{UV}}\Pi^{(2)} + L_{6D,5}^{\mathrm{UV}}\Pi^{(2)} + \delta m_2\Pi^{(6F,2*)},$$

$$\Pi^{(p39)} = \Delta\Pi^{(p39)} + B_{6G}^{\mathrm{UV}}\Pi^{(2)} + L_2^{\mathrm{UV}}\Pi^{(6D)} - L_2^{\mathrm{UV}}B_{4a}^{\mathrm{UV}}\Pi^{(2)} - 2(L_2^{\mathrm{UV}})^2\Pi^{(4b)} + 2(L_2^{\mathrm{UV}})^2B_2^{\mathrm{UV}}\Pi^{(2)} + L_{4b,2}^{\mathrm{UV}}\Pi^{(4b)}$$
$$- L_{4b,2}^{\mathrm{UV}}B_2^{\mathrm{UV}}\Pi^{(2)} + L_{4a,1}^{\mathrm{UV}}\Pi^{(4b)} - L_{4a,1}^{\mathrm{UV}}B_2^{\mathrm{UV}}\Pi^{(2)} + 2\delta m_2(L_2^{\mathrm{UV}})^2\Pi^{(2*)} - \delta m_2 L_{4b,2}^{\mathrm{UV}}\Pi^{(2*)} - \delta m_2 L_{4a,1}^{\mathrm{UV}}\Pi^{(2*)}$$
$$- \delta m_{4a}^{\mathrm{UV}}L_2^{\mathrm{UV}}\Pi^{(2*)} + \delta m_{6G}^{\mathrm{UV}}\Pi^{(2*)}.$$

APPENDIX D: DIVERGENCE STRUCTURE OF RENORMALIZATION CONSTANTS OF SIXTH AND LOWER ORDERS

Throughout this appendix $\tilde{L}_n$, $\tilde{B}_n$, and $\delta\tilde{m}_n$ denote quantities obtained by removing the overall UV divergences of L_n, B_n, and δm_n by the K operation. They may still have subdiagram UV divergences which are subtracted by subdiagram K operations. The resulting UV-finite quantities are denoted as L_n^R, B_n^R, and δm_n^R. These quantities may have IR divergences, which are subtracted by R subtraction and I subtraction. These operations create UV- and IR-finite quantities which are denoted as ΔL_n, ΔB_n, and $\Delta\delta m_n$.

1. Second-order renormalization constants

$$L_2 = L_2^{\mathrm{UV}} + \tilde{L}_2, \qquad L_2^R = \tilde{L}_2 = I_2,$$
$$B_2 = B_2^{\mathrm{UV}} + \tilde{B}_2, \qquad B_2^R = \tilde{B}_2 = -I_2 + \Delta B_2,$$
$$\Delta LB_2 = L_2^R + B_2^R = \Delta B_2, \qquad B_{2^*} = -2L_{2^*},$$
$$L_{2^*} = I_{2^*} + \Delta L_{2^*}, \qquad B_{2^{**}} = -2(2L_{2(1*1*)} + L_{2(1*2*)}),$$
$$\delta m_{2^*} = \delta m_{2^*}^{\mathrm{UV}} + I_2 + \Delta\delta m_{2^*}.$$

2. Fourth-order renormalization constants

$$\delta m_{4a}^R = \delta\tilde{m}_{4a},$$

$$\delta m_{4b}^R = \delta\tilde{m}_{4b} - \delta\tilde{m}_{2'} B_2^{\rm UV} - \delta\tilde{m}_{2*}\delta m_2,$$

$$\Delta\delta m_{4a} = \delta m_{4a}^R,$$

$$\Delta\delta m_{4b} = \delta m_{4b}^R,$$

$$\Delta\delta m_4 = \Delta\delta m_{4a} + \Delta\delta m_{4b},$$

$$B_{4a}^R = \tilde{B}_{4a} - 2L_2^{\rm UV}\tilde{B}_2,$$

$$B_{4b}^R = \tilde{B}_{4b} - \tilde{B}_{2'} B_2^{\rm UV} - \delta m_2 B_{2*},$$

$$L_{4a,1}^R = \tilde{L}_{4a,1} - \tilde{L}_2 L_2^{\rm UV},$$

$$L_{4a,2}^R = \tilde{L}_{4a,2},$$

$$L_{4b,1}^R = \tilde{L}_{4b,1} - \tilde{L}_{2'} B_2^{\rm UV} - \delta m_2 L_{2*},$$

$$L_{4b,2}^R = \tilde{L}_{4b,2} - \tilde{L}_2 L_2^{\rm UV},$$

$$\Delta LB_{4a} = B_{4a}^R + 2L_{4a,1}^R + L_{4a,2}^R,$$

$$\Delta LB_{4b} = B_{4b}^R + 2L_{4b,1}^R + L_{4b,2}^R - L_2^R B_2^R - (L_2^R)^2,$$

$$\Delta LB_4 = \Delta LB_{4a} + \Delta LB_{4b}.$$

3. Sixth-order renormalization constants

$$\begin{aligned}\delta m_{6A}^R = {}& \delta\tilde{m}_{6A} - B_2^{\rm UV}\delta\tilde{m}_{4b(1')} - B_2^{\rm UV}\delta\tilde{m}_{4b(3')} \\ & - 2\delta m_2 \delta\tilde{m}_{4b(1*)} + \delta\tilde{m}_{2''}(B_2^{\rm UV})^2 \\ & + \delta\tilde{m}_{2*'}\delta m_2 B_2^{\rm UV} + \delta\tilde{m}_{2*'}\delta m_2 B_2^{\rm UV} \\ & + \delta\tilde{m}_{2**}(\delta m_2)^2,\end{aligned}$$

$$\begin{aligned}\delta m_{6B}^R = {}& \delta\tilde{m}_{6B} - B_2^{\rm UV}\delta\tilde{m}_{4b(2')} - \delta m_2\delta\tilde{m}_{4b(2*)} - \delta\tilde{m}_{2'} B_{4b}^{\rm UV} \\ & + \delta\tilde{m}_{2'} B_{2'}^{\rm UV} B_2^{\rm UV} - \delta\tilde{m}_{2*}\delta m_{4b}^{\rm UV} + \delta\tilde{m}_{2*}\delta m_{2'}^{\rm UV} B_2^{\rm UV} \\ & + \delta\tilde{m}_{2*}\delta m_{2*}^{\rm UV}\delta m_2,\end{aligned}$$

$$\begin{aligned}\delta m_{6C}^R = {}& \delta\tilde{m}_{6C} - 2L_2^{\rm UV}\delta\tilde{m}_{4b} - \delta\tilde{m}_{2'} B_{4a}^{\rm UV} \\ & + 2\delta\tilde{m}_{2'} L_2^{\rm UV} B_2^{\rm UV} - \delta\tilde{m}_{2*}\delta m_{4a}^{\rm UV} \\ & + 2\delta\tilde{m}_{2*}\delta m_2 L_2^{\rm UV},\end{aligned}$$

$$\begin{aligned}\delta m_{6D}^R = {}& \delta\tilde{m}_{6D} - B_2^{\rm UV}\delta\tilde{m}_{4a(1')} - L_2^{\rm UV}\delta\tilde{m}_{4b} \\ & - \delta m_2\delta\tilde{m}_{4a(1*)} + \delta\tilde{m}_{2'} L_2^{\rm UV} B_2^{\rm UV} \\ & + \delta\tilde{m}_{2*}\delta m_2 L_2^{\rm UV},\end{aligned}$$

$$\delta m_{6E}^R = \delta\tilde{m}_{6E} - B_2^{\rm UV}\delta\tilde{m}_{4a(2')} - \delta m_2\delta\tilde{m}_{4a(2*)},$$

$$\delta m_{6F}^R = \delta\tilde{m}_{6F} - 2L_2^{\rm UV}\delta\tilde{m}_{4a},$$

$$\delta m_{6G}^R = \delta\tilde{m}_{6G} - L_2^{\rm UV}\delta\tilde{m}_{4a},$$

$$\delta m_{6H}^R = \delta\tilde{m}_{6H},$$

$$\Delta\delta m_{6A} = \delta m_{6A}^R,$$

$$\Delta\delta m_{6B} = \delta m_{6B}^R - \tilde{L}_2\delta m_{4b}^R,$$

$$\Delta\delta m_{6C} = \delta m_{6C}^R - \tilde{L}_2\delta m_{4a}^R,$$

$$\Delta\delta m_{6D} = \delta m_{6D}^R,$$

$$\Delta\delta m_{6E} = \delta m_{6E}^R,$$

$$\Delta\delta m_{6F} = \delta m_{6F}^R,$$

$$\Delta\delta m_{6G} = \delta m_{6G}^R,$$

$$\Delta\delta m_{6H} = \delta m_{6H}^R,$$

$$\begin{aligned}\Delta\delta m_6 = {}& \delta m_{6A}^R + \delta m_{6B}^R + \delta m_{6C}^R + 2\delta m_{6D}^R + \delta m_{6E}^R \\ & + \delta m_{6F}^R + 2\delta m_{6G}^R + \delta m_{6H}^R - \tilde{L}_2\delta m_{4a}^R \\ & - \tilde{L}_2\delta m_{4b}^R,\end{aligned}$$

$$\begin{aligned}B_{6A}^R = {}& \tilde{B}_{6A} - B_2^{\rm UV}\tilde{B}_{4b(1')} - B_2^{\rm UV}\tilde{B}_{4b(3')} + \tilde{B}_{2''}(B_2^{\rm UV})^2 \\ & - 2\delta m_2 B_{4b(1*)} + \delta m_2 B_2^{\rm UV} B_{2*'} + \delta m_2 B_2^{\rm UV} B_{2*'} \\ & + (\delta m_2)^2 B_{2**},\end{aligned}$$

$$\begin{aligned}B_{6B}^R = {}& \tilde{B}_{6B} - B_{2*}\delta m_{4b}^{\rm UV} - B_2^{\rm UV}\tilde{B}_{4b(2')} - \tilde{B}_{2'} B_{4b}^{\rm UV} \\ & + \tilde{B}_{2'} B_{2'}^{\rm UV} B_2^{\rm UV} - \delta m_2 B_{4b(2*)} + \delta m_{2'}^{\rm UV} B_2^{\rm UV} B_{2*} \\ & + \delta m_{2*}^{\rm UV}\delta m_2 B_{2*},\end{aligned}$$

$$\begin{aligned}B_{6C}^R = {}& \tilde{B}_{6C} - B_{2*}\delta m_{4a}^{\rm UV} - \tilde{B}_{2'} B_{4a}^{\rm UV} - 2L_2^{\rm UV}\tilde{B}_{4b} \\ & + 2L_2^{\rm UV}\tilde{B}_{2'} B_2^{\rm UV} + 2\delta m_2 L_2^{\rm UV} B_{2*},\end{aligned}$$

$$\begin{aligned}B_{6D}^R = {}& \tilde{B}_{6D} - B_2^{\rm UV}\tilde{B}_{4a(1')} - \tilde{B}_2 L_{4b,1}^{\rm UV} - L_2^{\rm UV}\tilde{B}_{4b} \\ & + L_2^{\rm UV}\tilde{B}_{2'} B_2^{\rm UV} + L_{2'}^{\rm UV}\tilde{B}_2 B_2^{\rm UV} - \delta m_2 B_{4a(1*)} \\ & + \delta m_2 L_2^{\rm UV} B_{2*},\end{aligned}$$

$$B^R_{6E} = \tilde{B}_{6E} - B^{\rm UV}_2 \tilde{B}_{4a(2')} - 2\tilde{B}_2 L^{\rm UV}_{4b,1} + L^{\rm UV}_{2'} \tilde{B}_2 B^{\rm UV}_2 + L^{\rm UV}_{2'} \tilde{B}_2 B^{\rm UV}_2 - \delta m_2 B_{4a(2*)},$$

$$B^R_{6F} = \tilde{B}_{6F} - 2\tilde{B}_2 L^{\rm UV}_{4a,1} - 2L^{\rm UV}_2 \tilde{B}_{4a} + 3(L^{\rm UV}_2)^2 \tilde{B}_2,$$

$$B^R_{6G} = \tilde{B}_{6G} - \tilde{B}_2 L^{\rm UV}_{4a,1} - \tilde{B}_2 L^{\rm UV}_{4b,2} - L^{\rm UV}_2 \tilde{B}_{4a} + 2(L^{\rm UV}_2)^2 \tilde{B}_2,$$

$$B^R_{6H} = \tilde{B}_{6H} - 2\tilde{B}_2 L^{\rm UV}_{4a,2},$$

$$L^R_{6A,1} = \tilde{L}_{6A,1} - B^{\rm UV}_2 \tilde{L}_{4b,1((1')')} - B^{\rm UV}_2 \tilde{L}_{4b,1(3')} + \tilde{L}_{2''}(B^{\rm UV}_2)^2 - \delta m_2 L_{4b,1((1')*)} - \delta m_2 L_{4b,1(3*)} + \delta m_2 L_{2*'} B^{\rm UV}_2 + \delta m_2 L_{2*'} B^{\rm UV}_2 + (\delta m_2)^2 L_{2(1*1*)},$$

$$L^R_{6A,2} = \tilde{L}_{6A,2} - B^{\rm UV}_2 \tilde{L}_{4b,2(3')} - L^{\rm UV}_2 \tilde{L}_{4b,1} + \tilde{L}_{2'} L^{\rm UV}_2 B^{\rm UV}_2 - \delta m_2 L_{4b,2(1*)} + \delta m_2 L^{\rm UV}_2 L_{2*},$$

$$L^R_{6A,3} = \tilde{L}_{6A,3} - 2B^{\rm UV}_2 \tilde{L}_{4b,1(1')} + \tilde{L}_{2''}(B^{\rm UV}_2)^2 - 2\delta m_2 L_{4b,1(1*)} + 2\delta m_2 L_{2*'} B^{\rm UV}_2 + (\delta m_2)^2 L_{2(1*(1')*)},$$

$$L^R_{6B,1} = \tilde{L}_{6B,1} - B^{\rm UV}_2 \tilde{L}_{4b,1(2')} - L_{2*} \delta m^{\rm UV}_{4b} - \tilde{L}_{2'} B^{\rm UV}_{4b} + \tilde{L}_{2'} B^{\rm UV}_{2'} B^{\rm UV}_2 - \delta m_2 L_{4b,1(2*)} + \delta m^{\rm UV}_{2'} L_{2*} B^{\rm UV}_2 + \delta m^{\rm UV}_{2*} \delta m_2 L_{2*},$$

$$L^R_{6B,2} = \tilde{L}_{6B,2} - B^{\rm UV}_2 \tilde{L}_{4b,2((2')')} - \tilde{L}_2 L^{\rm UV}_{4b,1} + \tilde{L}_2 L^{\rm UV}_{2'} B^{\rm UV}_2 - \delta m_2 L_{4b,2(2*)},$$

$$L^R_{6B,3} = \tilde{L}_{6B,3} - L^{\rm UV}_2 \tilde{L}_{4b,2} - \tilde{L}_2 L^{\rm UV}_{4b,2} + \tilde{L}_2 (L^{\rm UV}_2)^2,$$

$$L^R_{6C,1} = \tilde{L}_{6C,1} - L_{2*} \delta m^{\rm UV}_{4a} - 2L^{\rm UV}_2 \tilde{L}_{4b,1} - \tilde{L}_{2'} B^{\rm UV}_{4a} + 2\tilde{L}_{2'} L^{\rm UV}_2 B^{\rm UV}_2 + 2\delta m_2 L^{\rm UV}_2 L_{2*},$$

$$L^R_{6C,2} = \tilde{L}_{6C,2} - L^{\rm UV}_2 \tilde{L}_{4b,2} - \tilde{L}_2 L^{\rm UV}_{4a,1} + \tilde{L}_2 (L^{\rm UV}_2)^2,$$

$$L^R_{6C,3} = \tilde{L}_{6C,3} - \tilde{L}_2 L^{\rm UV}_{4a,2},$$

$$L^R_{6D,1} = \tilde{L}_{6D,1} - B^{\rm UV}_2 \tilde{L}_{4a,1((1')')} - L^{\rm UV}_2 \tilde{L}_{4b,1} + \tilde{L}_{2'} L^{\rm UV}_2 B^{\rm UV}_2 - \delta m_2 L_{4a,1((1')*)} + \delta m_2 L^{\rm UV}_2 L_{2*},$$

$$L^R_{6D,2} = \tilde{L}_{6D,2} - L^{\rm UV}_2 \tilde{L}_{4a,1} - L^{\rm UV}_2 \tilde{L}_{4b,2} + \tilde{L}_2 (L^{\rm UV}_2)^2,$$

$$L^R_{6D,3} = \tilde{L}_{6D,3} - B^{\rm UV}_2 \tilde{L}_{4a,1(1')} - L^{\rm UV}_2 \tilde{L}_{4b,1} + \tilde{L}_{2'} L^{\rm UV}_2 B^{\rm UV}_2 - \delta m_2 L_{4a,1(1*)} + \delta m_2 L^{\rm UV}_2 L_{2*},$$

$$L^R_{6D,4} = \tilde{L}_{6D,4} - B^{\rm UV}_2 \tilde{L}_{4a,2(1')} - \delta m_2 L_{4a,2(1*)},$$

$$L^R_{6D,5} = \tilde{L}_{6D,5} - B^{\rm UV}_2 \tilde{L}_{4a,1(3')} - \tilde{L}_2 L^{\rm UV}_{4b,1} + \tilde{L}_2 L^{\rm UV}_{2'} B^{\rm UV}_2 - \delta m_2 L_{4a,1(3*)},$$

$$L^R_{6E,1} = \tilde{L}_{6E,1} - B^{\rm UV}_2 \tilde{L}_{4a,1(2')} - \tilde{L}_2 L^{\rm UV}_{4b,1} + \tilde{L}_2 L^{\rm UV}_{2'} B^{\rm UV}_2 - \delta m_2 L_{4a,1(2*)},$$

$$L^R_{6E,2} = \tilde{L}_{6E,2} - B^{\rm UV}_2 \tilde{L}_{4a,2((2')')} - \delta m_2 L_{4a,2(2*)},$$

$$L^R_{6E,3} = \tilde{L}_{6E,3} - L^{\rm UV}_2 \tilde{L}_{4a,2},$$

$$L^R_{6F,1} = \tilde{L}_{6F,1} - L^{\rm UV}_2 \tilde{L}_{4a,1} - \tilde{L}_2 L^{\rm UV}_{4a,1} + \tilde{L}_2 (L^{\rm UV}_2)^2,$$

$$L^R_{6F,2} = \tilde{L}_{6F,2} - L^{\rm UV}_2 \tilde{L}_{4a,2},$$

$$L^R_{6F,3} = \tilde{L}_{6F,3} - 2L^{\rm UV}_2 \tilde{L}_{4a,1} + \tilde{L}_2 (L^{\rm UV}_2)^2,$$

$$L^R_{6G,1} = \tilde{L}_{6G,1} - L^{\rm UV}_2 \tilde{L}_{4a,1} - \tilde{L}_2 L^{\rm UV}_{4a,1} + \tilde{L}_2 (L^{\rm UV}_2)^2,$$

$$L^R_{6G,2} = \tilde{L}_{6G,2},$$

$$L^R_{6G,3} = \tilde{L}_{6G,3},$$

$$L^R_{6G,4} = \tilde{L}_{6G,4} - L^{\rm UV}_2 \tilde{L}_{4a,2},$$

$$L^R_{6G,5} = \tilde{L}_{6G,5} - L^{\rm UV}_2 \tilde{L}_{4a,1} - \tilde{L}_2 L^{\rm UV}_{4b,2} + \tilde{L}_2 (L^{\rm UV}_2)^2,$$

$$L^R_{6H,1} = \tilde{L}_{6H,1} - \tilde{L}_2 L^{\rm UV}_{4a,2},$$

$$L^R_{6H,2} = \tilde{L}_{6H,2},$$

$$L^R_{6H,3} = \tilde{L}_{6H,3},$$

$$\Delta LB_{6A} = B^R_{6A} + 2L^R_{6A,1} + 2L^R_{6A,2} + L^R_{6A,3} - 2\Delta LB_2 L^R_{4b,1},$$

$$\Delta LB_{6B} = B^R_{6B} + 2L^R_{6B,1} + 2L^R_{6B,2} + L^R_{6B,3} - \Delta LB_{4b} L^R_2 - \Delta LB_2 L^R_{4b,2},$$

$$\Delta LB_{6C} = B^R_{6C} + 2L^R_{6C,1} + 2L^R_{6C,2} + L^R_{6C,3} - \Delta LB_{4a} L^R_2,$$

$$\Delta LB_{6D} = B^R_{6D} + L^R_{6D,1} + L^R_{6D,2} + L^R_{6D,3} + L^R_{6D,4} + L^R_{6D,5} - \Delta LB_2 L^R_{4a,1},$$

$$\Delta LB_{6E} = B^R_{6E} + 2L^R_{6E,1} + 2L^R_{6E,2} + L^R_{6E,3} - \Delta LB_2 L^R_{4a,2},$$

$$\Delta LB_{6F} = B^R_{6F} + 2L^R_{6F,1} + 2L^R_{6F,2} + L^R_{6F,3},$$

$$\Delta LB_{6G} = B^R_{6G} + L^R_{6G,1} + L^R_{6G,2} + L^R_{6G,3} + L^R_{6G,4} + L^R_{6G,5},$$

$$\Delta LB_{6H} = B^R_{6H} + 2L^R_{6H,1} + 2L^R_{6H,2} + L^R_{6H,3},$$

$$\Delta LB_6 = \sum_{\beta=A}^{H} \lambda_\beta \Delta LB_{6\beta}, \quad \text{(D1)}$$

where $\lambda_A = \lambda_B = \lambda_C = \lambda_E = \lambda_F = \lambda_H = 1$, and $\lambda_D = \lambda_G = 2$.

ΔL_6 and ΔB_6 defined in Ref. [3] are related to ΔLB_6 through

$$\Delta LB_6 = \Delta L_6 + \Delta B_6 + \Delta L_4 \Delta B_2 + \Delta\delta m_4 B_{2^*}[I]. \quad \text{(D2)}$$

[1] D. Hanneke, S. Fogwell, and G. Gabrielse, Phys. Rev. Lett. **100**, 120801 (2008).

[2] D. Hanneke, S. Fogwell Hoogerheide, and G. Gabrielse, arXiv:1009.4831 [Phys. Rev. A (to be published)].

[3] T. Kinoshita and M. Nio, Phys. Rev. D **73**, 053007 (2006).

[4] T. Aoyama, M. Hayakawa, T. Kinoshita, and M. Nio, Phys. Rev. Lett. **99**, 110406 (2007).

[5] T. Aoyama, M. Hayakawa, T. Kinoshita, and M. Nio, Phys. Rev. D **77**, 053012 (2008).

[6] T. Teubner, K. Hagiwara, R. Liao, A. D. Martin, and D. Nomura, Proceedings of the PhiPsi09 Conference, 2009, Beijing, China.

[7] B. Krause, Phys. Lett. B **390**, 392 (1997).

[8] K. Melnikov and A. Vainshtein, Phys. Rev. D **70**, 113006 (2004).

[9] J. Bijnens and J. Prades, Mod. Phys. Lett. A **22**, 767 (2007).

[10] J. Prades, E. de Rafael, and A. Vainshtein, arXiv:0901.0306.

[11] A. Nyffeler, Phys. Rev. D **79**, 073012 (2009).

[12] M. Davier, A. Hoecker, B. Malaescu, and Z. Zhang, Eur. Phys. J. C **71**, 1515 (2011).

[13] M. Knecht, S. Peris, M. Perrottet, and E. De Rafael, J. High Energy Phys. 11 (2002) 003.

[14] A. Czarnecki, W. J. Marciano, and A. Vainshtein, Phys. Rev. D **67**, 073006 (2003); **73**, 119901(E) (2006).

[15] A. Czarnecki, B. Krause, and W. J. Marciano, Phys. Rev. Lett. **76**, 3267 (1996).

[16] R. Bouchendira, P. Clade, S. Guellati-Khelifa, F. Nez, and F. Biraben, Phys. Rev. Lett. **106**, 080801 (2011).

[17] P. J. Mohr, B. N. Taylor, and D. B. Newell, Rev. Mod. Phys. **80**, 633 (2008).

[18] T. Kinoshita and M. Nio, Phys. Rev. D **70**, 113001 (2004).

[19] T. Aoyama, M. Hayakawa, T. Kinoshita, and M. Nio, Nucl. Phys. **B740**, 138 (2006).

[20] T. Aoyama, M. Hayakawa, T. Kinoshita, and M. Nio, Nucl. Phys. **B796**, 184 (2008).

[21] T. Aoyama, M. Hayakawa, T. Kinoshita, M. Nio, and N. Watanabe, Phys. Rev. D **78**, 053005 (2008).

[22] T. Aoyama, M. Hayakawa, T. Kinoshita, and M. Nio, Phys. Rev. D **78**, 113006 (2008).

[23] T. Aoyama, K. Asano, M. Hayakawa, T. Kinoshita, M. Nio, and N. Watanabe, Phys. Rev. D **81**, 053009 (2010).

[24] T. Aoyama, M. Hayakawa, T. Kinoshita, and M. Nio, Phys. Rev. D **82**, 113004 (2010).

[25] T. Kinoshita, in *Quantum Electrodynamics*, edited by T. Kinoshita, Advanced Series on Directions in High Energy Physics Vol. 7 (World Scientific, Singapore, 1990), p. 218.

[26] A. L. Kataev, Phys. Lett. B **284**, 401 (1992).

[27] K. G. Chetyrkin, 9th Workshop Loops and Legs in Quantum Field Theory, http://indico.desy.de/conferenceDisplay.py?sessionId=1&contribId=14&confId=476 (2008), unpublished.

[28] P. A. Baikov, K. G. Chetyrkin, and C. Sturm, Nucl. Phys. B, Proc. Suppl. **183**, 8 (2008).

[29] B. E. Lautrup, A. Peterman, and E. de Rafael, Phys. Rep. **3**, 193 (1972).

[30] B. E. Lautrup and E. de Rafael, Phys. Rev. **174**, 1835 (1968).

[31] P. A. Baikov and D. J. Broadhurst, arXiv:hep-ph/9504398.

[32] T. Kinoshita and M. Nio, Phys. Rev. Lett. **82**, 3240 (1999).

[33] T. Kinoshita and M. Nio, Phys. Rev. D **60**, 053008 (1999).

[34] T. Aoyama, M. Hayakawa, T. Kinoshita, and M. Nio, Phys. Rev. D **83**, 053002 (2011).

[35] G. P. Lepage, J. Comput. Phys. **27**, 192 (1978).

[36] A. O. G. Kallen and A. Sabry, Kong. Dan. Vid. Sel. Mat. Fys. Med. **29N17**, 1 (1955).

[37] T. Kinoshita and M. Nio, Phys. Rev. D **73**, 013003 (2006).

[38] D. J. Broadhurst, A. L. Kataev, and O. V. Tarasov, Phys. Lett. B **298**, 445 (1993).

[39] T. Kinoshita, B. Nizic, and Y. Okamoto, Phys. Rev. D **41**, 593 (1990).

[40] T. Kinoshita, Phys. Rev. D **47**, 5013 (1993).